



Physikalisch-Technische Bundesanstalt  
Nationales Metrologieinstitut

## PriSpecTemp report: literature study on experimental line intensity of CO, CO<sub>2</sub> and O<sub>2</sub>

Lüttswager Alexandra<sup>1</sup>; Berezkin Kirill<sup>1</sup>; Li, Gang<sup>1</sup>; Castrillo Antonio<sup>2</sup>; Lisak Daniel<sup>3</sup>; Vainio Markku<sup>4</sup>; Uotila Touko<sup>4</sup>; Seppä Jeremias<sup>5</sup>

<sup>1</sup> PTB, Braunschweig, Germany.  <https://orcid.org/0000-0002-3934-6805>

 <https://orcid.org/0009-0000-8873-521X>

 <https://orcid.org/0000-0002-5605-7896>

<sup>2</sup> University of Campania "Luigi Vanvitelli", Caserta, Italy.

 <https://orcid.org/0000-0002-1253-9172>

<sup>3</sup> Nicolaus Copernicus University, Torun, Poland.  <https://orcid.org/0000-0001-5545-7989>

<sup>4</sup> University of Helsinki, Helsinki, Finland.  <https://orcid.org/0000-0002-9962-3827>

 [KPH-4522-2024](https://kph.fi/KPH-4522-2024)

<sup>3</sup> VTT, Espoo, Finland.  <https://orcid.org/0000-0002-6781-8443>

**DOI: [10.7795/120.20250221](https://doi.org/10.7795/120.20250221)**

**Veröffentlichungsjahr: 2025**

**Acknowledgement:** The project (22IEM03 PriSpecTemp) has received funding from the European Partnership on Metrology, co-financed from the European Union's Horizon Europe Research and Innovation Programme and by the Participating States.

**Angaben zum Urheberrecht:** open access

**Zitierform:** 22IEM03 PriSpecTemp, Activity 1.1.1: Intensities in CO, CO<sub>2</sub> and O<sub>2</sub> spectra, stand 2024". A. Lüttswager, K. Berezkin, G. Li A. Castrillo D. Lisak M. Vainio, T. Uotila, J. Seppä, DOI: [10.7795/120.20250221](https://doi.org/10.7795/120.20250221)



## 22IEM03 PriSpecTemp

### A1.1.1. Literature study on experimental line intensity of CO, CO<sub>2</sub> and O<sub>2</sub>

**Author names of the participants for the activity:**

A.V. Lüttschwager, K. Berezkin, G. Li (PTB)

A. Castrillo (SUN)

D. Lisak (UMK)

M. Vainio, T. Uotila (UH)

J. Seppä (VTT)

**Publication date:**

24.01.2025

<https://www.prispectemp.ptb.de>

**METROLOGY  
PARTNERSHIP**



The project (22IEM03 PriSpecTemp) has received funding from the European Partnership on Metrology, co-financed from the European Union's Horizon Europe Research and Innovation Programme and by the Participating States.

## Glossary

ABSCO	Calculated molecular absorption coefficients for a range of pressures, temperatures and H <sub>2</sub> O volume mixing ratios and stored in look-up tables
AMES	The NASA Ames PAH IR Spectroscopic Database
AMTS	Advanced Moisture and Temperature Sounder
CA-CRDS	Comb Assisted Cavity Ring-Down Spectroscopy
CDSD-296	High-resolution Carbon Dioxide Spectroscopic Databank
CMDS	Cavity Mode Dispersion Spectroscopy
CRD	Cavity Ring-Down
CRDS	Cavity Ring-Down Spectroscopy
DFB	Distributed-Feedback Laser
DLR	Deutsches Zentrum für Luft- und Raumfahrt (German Aerospace Center)
DMS	Dipole Moment Surface
DMF	Dipole Moment Function
FS-CRDS	Frequency Stabilized Cavity Ring-Down Spectroscopy
FTIR	Fourier-Transform Infrared Spectroscopy
FTS	Fourier-Transform Spectroscopy
ILS technique	Intracavity Laser Spectroscopy (not to be confused with ILS – instrumental line shape)
GEISA	Gestion et Etude des Informations Spectroscopiques Atmosphériques (Database)
HITRAN	High-resolution transmission molecular absorption database (Spectroscopic database)
HR	High Resolution
HTP	Hartmann-Tran Profile (spectral profile named after its inventors)
IUPAC	International Union of Pure and Applied Chemistry
MIR	Middle Infrared Region
NICE-OHMS	Noise-Immune Cavity-Enhanced Optical Heterodyne Molecular Spectroscopy
NIR	Near Infrared Region
NIST	National Institute of Standards and Technology
RVSGT	Rotational–Vibrational Spectroscopic Gas Thermometry
TDLAS	Tuneable Diode Laser Absorption Spectroscopy

## TABLE OF CONTENTS

A1.1.1. Literature study on experimental line intensity of CO, CO <sub>2</sub> and O <sub>2</sub> .....	1
1 Summary .....	4
2 Introduction .....	4
3 Carbon monoxide, CO .....	4
3.1 Line intensity of CO at 4.5 $\mu\text{m}$ .....	5
3.2 Line intensity of CO at 2.3 $\mu\text{m}$ .....	6
3.3 Line intensity of CO at 1.57 $\mu\text{m}$ .....	7
Carbon dioxide, CO <sub>2</sub> .....	9
3.4 Line intensity of CO <sub>2</sub> at 4.3 $\mu\text{m}$ .....	9
3.5 Line intensity of CO <sub>2</sub> at 2.8 $\mu\text{m}$ .....	10
3.6 Line intensity of CO <sub>2</sub> near 2 $\mu\text{m}$ .....	12
3.7 Line intensity of CO <sub>2</sub> at 1.60 $\mu\text{m}$ and 1.57 $\mu\text{m}$ .....	14
4 Oxygen, O <sub>2</sub> .....	16
4.1 A-band of O <sub>2</sub> (0.76 $\mu\text{m}$ ) .....	16
5 References .....	19

# 1 Summary

This report is an overview of the existing literature sources for the atmospheric “sensor” molecules (CO, CO<sub>2</sub>, O<sub>2</sub>). Existing accurate measurements of the **line intensity** in different frequency ranges (molecular bands), suitable for both highly accurate *ab initio* calculations, measurements, and specification of the reference temperatures are targeted. The document is partitioned as follows: after a brief introduction in the second section, 3<sup>rd</sup>, 4<sup>th</sup> and 5<sup>th</sup> sections are dedicated to carbon monoxide, carbon dioxide and molecular oxygen, respectively. Information about the bands is collected in subsections. In case of CO, CO<sub>2</sub>, vibrational excitation determines the partition within a subsection: the bands with low excitation are mentioned first. For the oxygen molecule only electronic A-band is considered.

## 2 Introduction

Small molecules containing oxygen are ever-present atmospheric constituents, reflecting functioning of the planet. An equilibrium between CO<sub>2</sub> and O<sub>2</sub> tells primarily about the efficiency of photosynthesis counterweighting the breath, and CO reflects an incomplete burn of carbon-containing substances (fuels or forests).

In the gas phase, absorption spectra of light molecules such as CO<sub>2</sub>, O<sub>2</sub> and CO consist of groups of spectral features (bands) with regular structure (see. Figure 3-4, Figure 0-1 and Figure 4-1). Integrated intensities of different bands decrease with increasing excitation. Knowing the intensities of low frequency fundamental transitions, which absorb in the range of the Earth’s infrared emission interval is helpful for determining the impact of a molecule on the global warming. These are normally highly absorbing transitions which require small absorption path and concentrations. High overtones (or weak forbidden bands as it is the case with O<sub>2</sub>) are useful for the atmospheric sensing.

Knowledge of the structure or/and intensities of spectral bands is a necessary input for theoretical calculations, which yield essential molecular parameters, such as dipole moment function, Hermann-Wallis coefficients, Coriolis coupling constants, broadening and shifting coefficients, etc. Molecular constants, in turn, make possible the modelling of any band at different temperatures, regardless of its accessibility by an experiment.

Whereas molecular constants determine the probability of a transition between energy levels, the temperature influences the population of the levels of the initial state, causing intensity redistribution between different lines within an absorption band.

Therefore, the absolute value of the intensities is of a secondary importance for the temperature determination, but the accurate knowledge of the ratios between different lines is essential.

## 3 Carbon monoxide, CO

Carbon monoxide is one of the most studied molecules because of its small size (hence accessibility of extensive theoretical treatment) and the involvement in many anthropogenic and natural processes on Earth.

The CO molecule was included in the HITRAN database since its very first version to aid the remote sensing of the terrestrial atmospheric CO. A major update was made in HITRAN 2016 [1], largely based on the work of Li et al. [2]. In this work, a semi-empirical dipole moment function (DMF) was derived from appropriately weighted experimental line intensities in literature and two CRDS measurements of the 4←0 [2] and 6←0 band [3]. Combined with the potential energy surface (PEC) from Coxon and Hajigeorgiou [4], ro-vibrational line intensities of the 0←0 to 7←0 bands were derived. In the latest version of HITRAN (HITRAN 2020) [5], the line intensities of the 1←0 and 3←0 bands have been updated [6] using scaling factors of 1.02 and 1.026, respectively, derived from the measurements and calculations [7,8,27].

CO is also a molecule routinely monitored in many industrial processes, some of them involving high temperatures. For this reason, the HITEMP database [9] (high-temperature analogue of HITRAN) includes

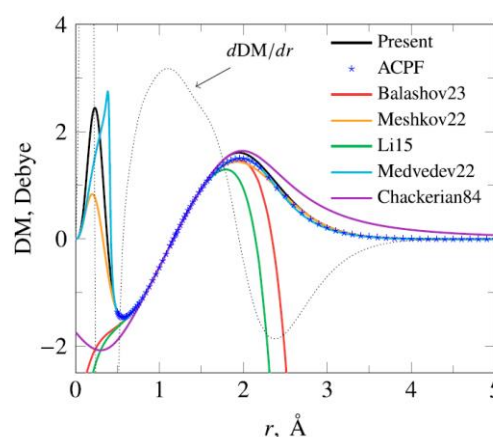


Figure 3-1. Dipole moment function of the ground state of CO, taken from Ref. [15] (Figure 1).

higher vibrational bands and rotational lines, whose intensities become significant with increasing temperature. The current CO line list in the HITEMP2010 database [9] is largely based on Refs. [10, 11], supplemented with the values from Cologne Database for Molecular Spectroscopy (CDMS) [12] in the MW region and experimental data for the overtone bands  $2\leftarrow 0$  and  $3\leftarrow 0$  from [13] and [14], respectively. It consists of 113631 lines, with  $v_{max} = 20$  and  $J_{max} = 150$ , where  $v$ ,  $J$  are vibrational and rotational quantum numbers, respectively.

The dipole moment function is a key physical property to access the infrared intensities (in dipole approximation). For carbon monoxide it is unusual: it does not stay positive for all bond lengths like in hydrogen halides family, but changes sign in the vicinity of the equilibrium bond length (1.128 Å), see Figure 3-1 (the latter is taken from Ref. [15]). Measurements in the microwave and IR regions allow reconstruction of the dipole moment function in an interval of c.a. 1 Å, centered at the equilibrium bond length. A polynomial expansion, obtained from experimental values in Ref. [2] and used in HITRAN16 [1] is shown in green in Figure 3-1. One can see that the polynomial representation exhibits non-physical behavior with increasing or decreasing bond length. Adding information on high overtone,  $7\leftarrow 0$  (Ref. [16], red curve on Figure 3-1) expands the interval. Significant effort is put into the generation of an empirical dipole moment function, which not only reproduces the experimental values, but has correct asymptotes [17, 18]. Regardless of all the efforts invested by both theoreticians and experimentalists, new unresolved issues pop-up [15].

In the following sub-sections, a part of relatively recent articles is listed where the experiments are performed on a similar technical (and modern) level. Most or earlier works can be found in the references of the articles cited here.

### 3.1 Line intensity of CO at 4.5 $\mu\text{m}$

CO fundamental band at 4.5  $\mu\text{m}$  is the strongest absorption feature this molecule has. High intensity makes it difficult to measure accurately. The measurement requires strong control over small partial pressures (high dilutions) and absorption paths. Nevertheless, the band is successfully investigated. A very extensive study on the line parameters of both, fundamental and first overtone bands were performed by Zou and Varanasi back in 2002 [19]. Several broadband spectra at different pressures and temperatures (down to 174 K) were recorded. Spectral parameters were extracted by multi-spectrum fitting procedure. Voigt profile was accepted as a line shape model, the instrument function was considered as well.

Work by A. Predoi-Cross et al. [21] was performed using a similar instrumentation as in Ref. [19], but more advance fitting functions (line profiles) were applied, which lead to a significant lowering of the uncertainties. Ref. [19] clearly demonstrates, that accounting for the speed dependence and line mixing is necessary, and a simple symmetric Voigt function does not provide an accurate description of the line shape. This approach was later expanded to a larger  $J$ -interval as well as to three CO isotopologues in Ref. [7].

Table 1. Summary of the experimental works, focused on the intensity measurements in the fundamental band of CO. Relative uncertainties in the last column correspond to a standard deviation ( $k = 1$ ).

Reference	Year	Technique	Transitions/Bands	Isotopologue	$u(S)/S$ (%)
[19]	2002	FTIR	P <sub>23</sub> -R <sub>25</sub>	<sup>12</sup> C <sup>16</sup> O	~ 0.5 for strong lines
[20]	2007	TDLAS	R <sub>9</sub> , R <sub>10</sub> , R <sub>17</sub> , R <sub>18</sub>	<sup>12</sup> C <sup>16</sup> O	4 (only for R <sub>9</sub> , R <sub>10</sub> )
[21]	2016	FTIR	P <sub>22</sub> -R <sub>22</sub>	<sup>12</sup> C <sup>16</sup> O	Fit uncertainties below 0.1
[7]	2018	FTIR	P <sub>33</sub> -R <sub>38</sub>	<sup>12</sup> C <sup>16</sup> O  <sup>13</sup> C <sup>16</sup> O, <sup>12</sup> C <sup>18</sup> O, <sup>13</sup> C <sup>18</sup> O	0.04 at $m = 20$ to 0.07 at $m = 30$ , less than 0.15% for $m = 40$  1-2%
[22]	2023	TDLAS	P <sub>20</sub>	<sup>12</sup> C <sup>16</sup> O	3

Laser-based measurements of P<sub>20</sub> in [22] and R<sub>9</sub>, R<sub>10</sub> [20] yielded intensity with 3% and 4% uncertainty, respectively. It is a much larger value than a typical multi-spectrum fit of a full band [7, 19, 21] can provide, but the measurements remain an important cross-check between different methods.

It is worth noting, that Table 1 in Ref. [22] is a good reference source of the experimental works dedicated to the development of a laser-based CO sensor.

### 3.2 Line intensity of CO at 2.3 $\mu\text{m}$

First overtone of CO was measured essentially by the broadband FT-based techniques. Relatively recent publications, reporting experimental intensities, are listed in Table 2.

Table 2. Summary of the experimental works, focused on the intensity measurements in the first overtone of CO. Relative uncertainties in the last column correspond to a standard deviation ( $k = 1$ ).

Reference	Year	Technique	Transitions/Bands	Isotopologue	$u(S)/S$ (%)
[19]	2002	FTIR	P <sub>24</sub> -R <sub>23</sub>	<sup>12</sup> C <sup>16</sup> O	~ 0.7 for strong lines
[13]	2003	FTIR	P <sub>23</sub> -R <sub>22</sub>	<sup>12</sup> C <sup>16</sup> O	0.026 for integrated intensity at 296 K*
[23]	2012	FTIR	P <sub>29</sub> -R <sub>29</sub> P <sub>29</sub> -R <sub>29</sub>	<sup>12</sup> C <sup>16</sup> O <sup>13</sup> C <sup>16</sup> O, <sup>12</sup> C <sup>18</sup> O, <sup>13</sup> C <sup>18</sup> O	0.05 for $ m  < 20^{**}$ Announced to be published later
[24]	2017	FTIR	P <sub>24</sub> -R <sub>23</sub>	<sup>2</sup> C <sup>16</sup> O	0.05 for strong lines

\* Ref [13] reports only standard deviations of transition dipole moments, which are, possibly, do not contain cross-correlations with other parameters and appear underestimated (order of magnitude of 0.005%).

Ref. [19] reports not only a large set of spectroscopic parameters for the fundamental band, but for the first overtone as well. Work by Brault et al. [13] on self-broadening and shifting of CO, which followed Ref. [19] in quick succession, reported a new set of HR spectra at room temperatures, and an observation that the line asymmetries (deviations from Voigt profiles) cannot be ignored if high accuracies are targeted. A long list of line profiles was used, stating the importance of speed dependence and line mixing for the modelling. Intensities in Ref. [19] are 4.2% smaller than in the contemporary version of HITRAN, which lead to the 2004 update to CO line list in HITRAN 2004. All following studies use asymmetric profiles.

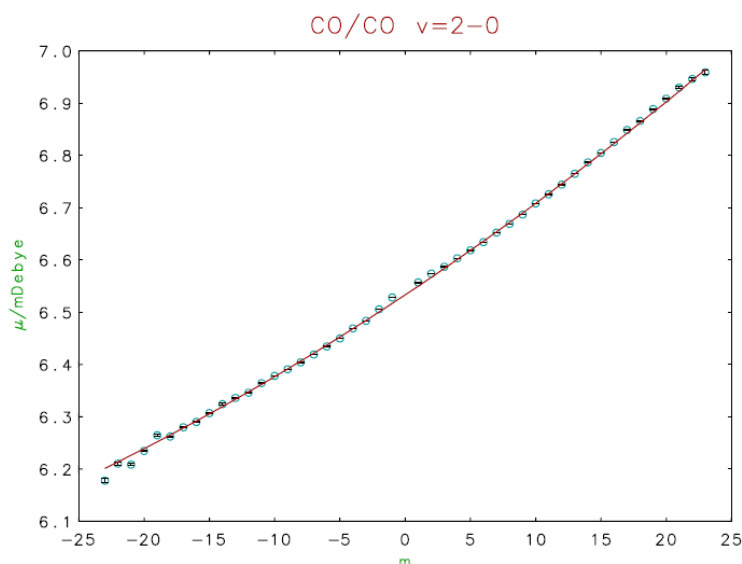


Figure 3-2 Transition moments for the second overtone; open circles retrieved from multispectrum fit, line from Herman–Wallis factor fit. The figure is copied from Ref. [[13]]

Recently Reed et al. had shown [29] that there is an effect of intensity depletion for the low J lines in the second overtone due to the intermolecular interaction (inelastic collisions). Figure 1 in Ref. [28] is another representation of the same difference between the calculations of a free molecule and experimental results. The same effect should be detectable for all other bands, and it is: upon an inspection of Figure 5 in [13], one can see that the dipole matrix elements in the band centre deviate very slightly, but systematically for the Herman-Wallis parabolic fit. Such behaviour is typical for many molecules, for example, for hydrogen halides, but it remains devoid of attention for the most systems

A very extensive study by Devi et al. [23] uses two spectrometers, different cells, pressures and temperatures, as well as sample compositions (neat gas and air-broadened CO, different isotopic enrichment). Total of 26 spectra were fitted simultaneously. The authors state that the usage of all data set was essential for the low uncertainty of the derived parameters.

The manuscript by Esteki et al. [24] focuses primarily on shifting and broadening coefficients at 298 K in the first overtone, but it reports the line strengths as well. It is shown that speed-dependent Voigt profile yields smaller uncertainties. The authors, similar to Refs. [13] and [23], claim achieving intensities below  $\sim 0.05\%$ . One should note that all works, mentioned here (Table 2), report deviations among them and major databases, which go above uncertainty margins. In Ref. [24] the deviations for the reported intensities amount to c.a. 1.01 for HITRAN 2012 and 0.94 for GEISA 2015 [25]. It shows that regardless of the efforts, there are still some unresolved issues.

### 3.3 Line intensity of CO at 1.57 $\mu\text{m}$

Second overtone (Figure 3-4) is often subjected to experimental investigations. A selection of recent studies involving intensity analysis is listed in Table 3. Older works can be found in the reference sections of articles in Table 3.

The overtone band is still in the range of frequencies, where conventional FT spectrometers are efficient. Due to the band's weakness, long absorption paths and relatively high pressures are needed, both of which are easier to control or determine than those parameters, necessary for the absorption measurements in the fundamental region. It means that smaller uncertainties can be reached. In the broadband study of the main isotopologue by Sung et al. [14] the path of 12.8 m is used whereas a recent article by Borkov et al. [27] a multi-pass cell with 30 m base tuned up to 1.057 km. As a results Ref. [27] reports the results for six isotopologues of CO as well as the hot transition ( $4\leftarrow 1$ ).

The vibrational frequency is high enough that the laser-based methods can be applied [8, 26, 28, 29, 30]. It gives a possibility of cross-checking the results, obtained by different techniques, which helps to pinpoint technique-related biases. An impressive example of such intercomparison, enriched by ab initio calculations is Ref. [28], where the results of experimental studies as well as the calculations agree on the level of 0.1%. In all cases the measurements were performed at the temperatures, close to 298 K. Experimental values can be found in the supplemental material to this article [28].

High accuracy of the spectral data in 1.57  $\mu\text{m}$  region allowed Reed et al. [29] to investigate the impact of intermolecular interactions on intensities of free molecules even at the sub atmospheric pressures. Line intensities (area under the lines) were shown to decrease with rising pressure of nitrogen and remain constant in case helium was used as a buffer gas (see Figure 3-3, which is also Figure 1 in [29]). It complies with the stronger interaction of CO with nitrogen due to the presence of quadrupole moment and a larger polarizability than those of He. The lines with small rotational quantum numbers affected in a larger extent, since the anisotropy of the interactions is more pronounced. Similar effects were observed during the past decades for many absorbers and perturbers, but at significantly higher

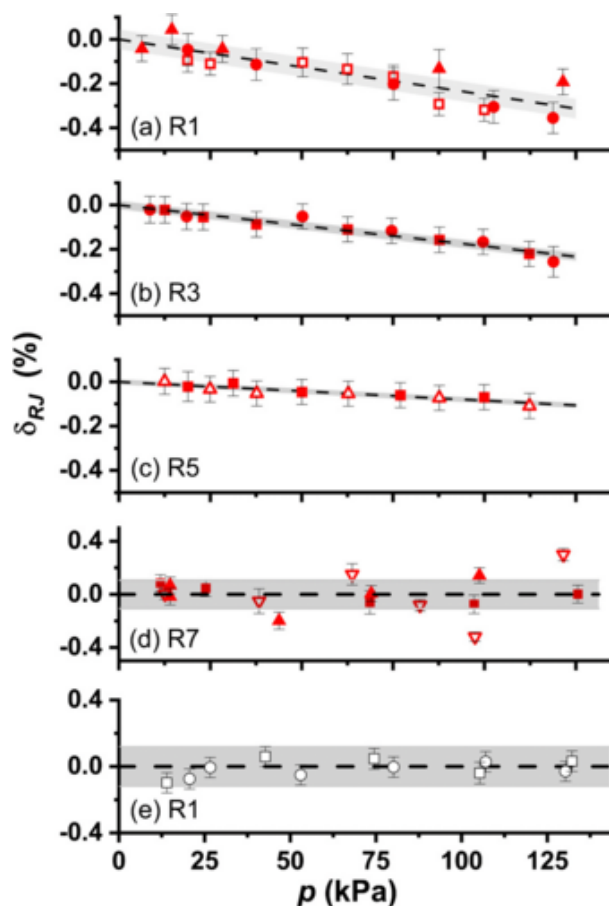


Figure 3-3. Pressure dependence of the relative differences in the integrated line shapes for ( $3\leftarrow 0$ ) band R-branch transitions of CO, taken from Ref. [29].



pressures. Now the technology allows to see it (and subsequently take account) even at typical atmospheric conditions.

Table 3. Summary of the experimental works, focused on the intensity measurements in the second overtone of CO. Relative uncertainties in the last column correspond to a standard deviation ( $k = 1$ ).

Reference	Year	Technique	Transitions/Bands	Isotopologue	u(S)/S (%)
[14]	2004	FTIR	P <sub>25</sub> to R <sub>25</sub>	<sup>12</sup> C <sup>16</sup> O	0.1-0.7 (at 298 K)
[26]	2013	FS-CRDS	P <sub>27</sub> , P <sub>28</sub> P <sub>14</sub> , P <sub>15</sub> of (4←1) R <sub>0</sub> -R <sub>2</sub> P <sub>15</sub> , P <sub>14</sub> P <sub>1</sub> , P <sub>2</sub>	<sup>12</sup> C <sup>16</sup> O <sup>12</sup> C <sup>16</sup> O <sup>12</sup> C <sup>18</sup> O <sup>12</sup> C <sup>17</sup> O <sup>13</sup> C <sup>16</sup> O	0.6 in most cases
[8]	2019	CMDS	R <sub>23</sub>	<sup>12</sup> C <sup>16</sup> O	0.07
[27]	2020	FTIR	Up to J=41 for <sup>12</sup> C <sup>16</sup> O	<sup>12</sup> C <sup>16</sup> O, <sup>13</sup> C <sup>16</sup> O, <sup>12</sup> C <sup>18</sup> O, <sup>12</sup> C <sup>17</sup> O, <sup>13</sup> C <sup>18</sup> O, <sup>13</sup> C <sup>17</sup> O (in natural abundance)	2-2.5 for strong unsaturated lines of <sup>12</sup> C <sup>16</sup> O
[28]	2022	CMDS CRDS FTIR	P <sub>27</sub> , R <sub>23</sub> , R <sub>26</sub> -R <sub>29</sub> P <sub>27</sub> , R <sub>23</sub> , R <sub>26</sub> -R <sub>29</sub> P <sub>22</sub> -R <sub>22</sub>	<sup>12</sup> C <sup>16</sup> O	0.1-0.12 NCU 0.09-0.18 NIST 0.13 PTB
[29]	2023	CRDS	R <sub>1</sub> , R <sub>3</sub> , R <sub>5</sub> , R <sub>7</sub>	<sup>12</sup> C <sup>16</sup> O	<0.1
[30]	2024	CRDS CMDS	R <sub>23</sub> , R <sub>25</sub> -R <sub>31</sub>	<sup>12</sup> C <sup>16</sup> O	0.07 for R <sub>27</sub> , 0.08 for R <sub>27</sub>

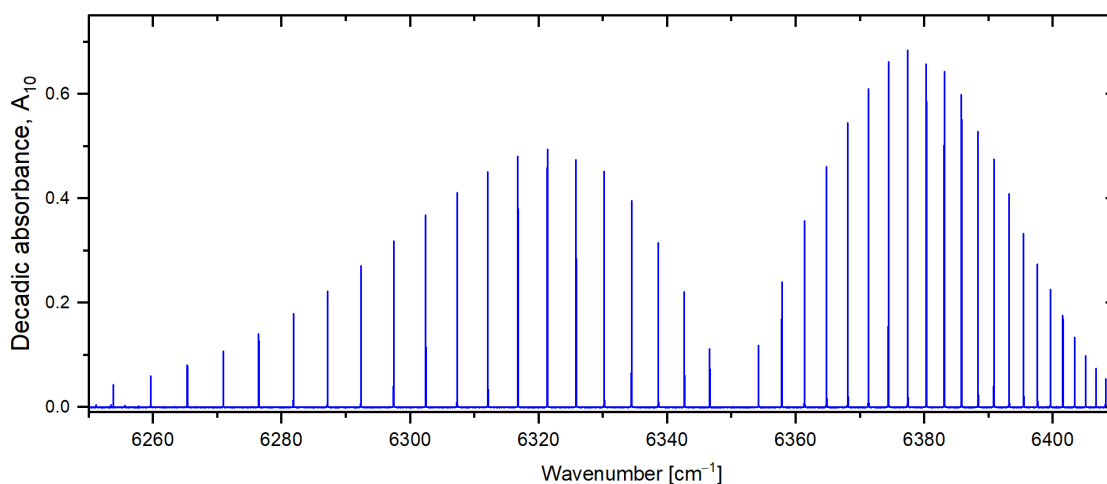


Figure 3-4. Spectrum of the second overtone of CO at 300 K, measured at PTB during PriSpecTemp project.

## Carbon dioxide, CO<sub>2</sub>

Carbon dioxide is a linear molecule with three vibrational modes, two of them are IR-active. Upon increasing of the number of vibrational modes, the spectrum becomes significantly more complicated. Combination and difference and hot bands can be observed. Frequencies and intensities can be affected by Fermi and Darling-Dennison resonances and Coriolis interaction. The spectra are more congested; hence the line mixing effect is more pronounced.

### 3.4 Line intensity of CO<sub>2</sub> at 4.3 $\mu\text{m}$

The  $\nu_3$  fundamental band of CO<sub>2</sub> at 4.3  $\mu\text{m}$  (around 2350  $\text{cm}^{-1}$ ) is an antisymmetric stretching vibration. In the notation scheme used in the HITRAN database [5] it can be represented as (00<sup>0</sup>11 $\leftarrow$ 00<sup>0</sup>01). At room temperature the hot bands ( $\nu_2 + \nu_3$ ) -  $\nu_2$  and ( $\nu_1 + \nu_3$ ) -  $\nu_1$  (HITRAN notation: 01<sup>1</sup>11 $\leftarrow$ 01<sup>1</sup>01 and 10<sup>0</sup>11 $\leftarrow$ 10<sup>0</sup>01, respectively) are also visible. Some literature sources reported also intensities of the strongest bands (mostly  $\nu_3$ ) for various isotopologues (<sup>13</sup>C<sup>16</sup>O<sub>2</sub>, <sup>12</sup>C<sup>16</sup>O<sup>18</sup>O, <sup>12</sup>C<sup>16</sup>O<sup>17</sup>O). The current edition of HITRAN database states the uncertainty codes of intensities of the fundamental band in the discussed region being 7 (i.e.,  $\geq 1\%$  and  $< 2\%$ ).

Current HITRAN version mainly relies on CDSD-296 [31,32] (high resolution Carbon Dioxide Spectroscopic Databank). In turn, CDSD-296 contains the data, generated within the framework of the method of effective operators and based on the global weighted fits of spectroscopic parameters (parameters of the effective Hamiltonians and effective dipole moment operators) retrieved from the experimental data collected from the literature. The reference temperature is 296 K, and the intensity cutoff is 10<sup>-30</sup>  $\text{cm}^{-1}/(\text{molecule cm}^{-2})$ .

Table 4 lists the literature sources, reporting the line intensities of CO<sub>2</sub> in the region around fundamental band at 4.3  $\mu\text{m}$  in chronological order. One can notice from the last column, that the relative uncertainties are rather high. It results from the difficulty of controlling small pressures and pathlength which are necessary for the measurement of a strongly absorbing transition like  $\nu_3$  fundamental band.

Table 4. Summary of the experimental works performed in the proximity of 4.3  $\mu\text{m}$  band, in which the line strengths of CO<sub>2</sub> transitions have been determined.

Ref.	Year	Technique	Bands	Number of transitions	Iso.	$\Delta S/S$ , %
[33]	1972	Grating IR	00 <sup>0</sup> 11 $\leftarrow$ 00 <sup>0</sup> 01	25	626	~10-16%
[34]	1977	TDLAS	00 <sup>0</sup> 11 $\leftarrow$ 00 <sup>0</sup> 01	1	636	12 %
				3	646	13-22 %
[35]	1980	Grating IR	00 <sup>0</sup> 11 $\leftarrow$ 00 <sup>0</sup> 01	23	626	5-10 %
[36]	1980	Grating IR	00 <sup>0</sup> 11 $\leftarrow$ 00 <sup>0</sup> 01 01 <sup>1</sup> 11 $\leftarrow$ 01 <sup>1</sup> 01	34	636	~10 %
[37]	1984	TDLAS	10 <sup>0</sup> 12 $\leftarrow$ 10 <sup>0</sup> 02	39	626	~3 %
			01 <sup>1</sup> 11 $\leftarrow$ 01 <sup>1</sup> 01		628	
			00 <sup>0</sup> 11 $\leftarrow$ 00 <sup>0</sup> 01		627	
[38]	1986	AMT	00 <sup>0</sup> 11 $\leftarrow$ 00 <sup>0</sup> 01	14	626	~3 %
[39]	1987	FTIR	00 <sup>0</sup> 11 $\leftarrow$ 00 <sup>0</sup> 01	340	626	~2 %
			01 <sup>1</sup> 11 $\leftarrow$ 01 <sup>1</sup> 01		636	
			02 <sup>2</sup> 11 $\leftarrow$ 02 <sup>2</sup> 01		628	
			10 <sup>0</sup> 11 $\leftarrow$ 10 <sup>0</sup> 01		627	
[40]	1988	Diode Laser (high temp)	10 <sup>0</sup> 11 $\leftarrow$ 10 <sup>0</sup> 01	3	626	~2.5 %
[41]	1989	FTIR	00 <sup>0</sup> 11 $\leftarrow$ 00 <sup>0</sup> 01	23	626	~2 %
				17	636	

[42]	1991	Diode Laser (high temp)	00 <sup>0</sup> 11←00 <sup>0</sup> 01	1 ( <sup>12</sup> C) + 4 ( <sup>13</sup> C)	626 636	~3 %
			01 <sup>1</sup> 11←01 <sup>1</sup> 01	5		
			10 <sup>0</sup> 12←10 <sup>0</sup> 02	2		
			02 <sup>2</sup> 11←02 <sup>2</sup> 01	5		
			10 <sup>0</sup> 11←10 <sup>0</sup> 01	2		
			11 <sup>1</sup> 12←11 <sup>1</sup> 02	4		
			03 <sup>3</sup> 11←03 <sup>3</sup> 01	5		
			11 <sup>1</sup> 11←11 <sup>1</sup> 01	6		
[43]	1993	Diode Laser (high temp)	12 <sup>2</sup> 12←12 <sup>2</sup> 02	4	626      636	~2-3 %
			20 <sup>0</sup> 13←20 <sup>0</sup> 03	3		
			20 <sup>0</sup> 12←20 <sup>0</sup> 02	3		
			12 <sup>2</sup> 11←12 <sup>2</sup> 01	3		
			20 <sup>0</sup> 11←20 <sup>0</sup> 01	2		
			01 <sup>1</sup> 21←01 <sup>1</sup> 01	5		
			01 <sup>1</sup> 11←01 <sup>1</sup> 01	4		
[44]	1994	FTIR	00 <sup>0</sup> 11←00 <sup>0</sup> 01	19	626	~3-16 % (various temperatures)
[45]	1998	FTIR	00 <sup>0</sup> 11←00 <sup>0</sup> 01	15	627	~3-5%
				18	637	
[46]	1998	FTIR	00 <sup>0</sup> 11←00 <sup>0</sup> 01	75	627	~3 %
			01 <sup>1</sup> 11←01 <sup>1</sup> 01			
[47]	2008	FTIR	10 <sup>0</sup> 11←10 <sup>0</sup> 01	135  128	638  838	1-10 % (wide range measured)
			02 <sup>2</sup> 11←02 <sup>2</sup> 01			
			01 <sup>1</sup> 11←01 <sup>1</sup> 01			
			00 <sup>0</sup> 11←00 <sup>0</sup> 01			
[48]	2012	FTIR	00 <sup>0</sup> 11←00 <sup>0</sup> 01  01 <sup>1</sup> 11←01 <sup>1</sup> 01	37	626	~3 %
				15	628	~3 %
				64	627	~5 %
				18	728	~3 %

Important note from Ref. [10]: “Errors in the temperature <...> affect the intensities in a more complex manner. It can be shown that an error of 1 K at 300 K affects CO<sub>2</sub> intensity measurements by -0.6% at J = 40, by -1.9% at J = 60, by -3.8% at J = 80, and by -5% at J = 90”.

### 3.5 Line intensity of CO<sub>2</sub> at 2.8 μm

In the spectral region around 2.8 μm (usually between 3450 and 3750 cm<sup>-1</sup> in terms of wavenumbers), the CO<sub>2</sub> absorption bands belong to the so-called DP = 5 polyad. Among all the possible bands of this polyad, two are relatively strong combination bands (the 10<sup>0</sup>11←00<sup>0</sup>01 and 10<sup>0</sup>12←00<sup>0</sup>01, in the HITRAN notation), while the others are hot bands, having the 11<sup>1</sup>12←01<sup>1</sup>01 a relatively strong band intensity. In the case of the most abundant isotopologue (<sup>16</sup>O<sup>12</sup>C<sup>16</sup>O, or 626 in the HITRAN notation), the two combination bands have band intensities that are in the order of 1·10<sup>-18</sup> cm/molecule.

In the latest version of the HITRAN database (HITRAN2020 [5]), the line strength (S) values provided for all the bands of this spectral region (for all the isotopologues) come from theoretical (*ab-initio*) calculations [49].

For the 626 isotopologue, they come from the calculations performed by the University College of London group and by the V.E. Zuev Institute of Atmospheric Optics group. In HITRAN, the uncertainty given for these S-values are in the range 1-5%, in relative terms.

Like HITRAN, also other available databases, such as CDSD-296 [31,32], GEISA [25], or AMES, provide line strength values that are based on theoretical calculations.

Table 5 Summary of the experimental works performed around 2.8  $\mu\text{m}$ , in which the line strengths of CO<sub>2</sub> transitions have been determined.

Reference	Year	Technique	Number of Bands	Number of transitions	Isotopologue*	u(S)/S (%)**
[50]	1988	FTIR	4	180	626	2
[41]	1989	FTIR	4	180	626	2
[51]	1998	FTIR	36	~1500	626	0.5-40
[52]	2004	FTIR	12	453	626	<10
[48]	2012	FTIR	4	693	626, 627, 727, 628, 728, 828, 636, 637, 638	3-15
[53]	2008	TDLAS	2	2	626	2
[54]	2013	TDLAS	1	2	626	~0.6
[55]	2007	FTIR	44	>3700	628, 828, 728	1-10
[47]	2008	FTIR	41	>2000	636, 638, 637, 838	1-10

\*This information is reported in HITRAN notation. \*\*1- $\sigma$  ( $k = 1$ ) confidence level.

As far as experimental S data are concerned, it is important to point out that there are only few works that provide reliable data. The first data have been obtained in the period 1988-1989 by scientists at the National Research Council of Canada [50,41]. With their experimental work, based on the use of Bomen spectrophotometer, absorption spectra from about 3300 to 4000  $\text{cm}^{-1}$  were recorded, so investigating a total of four bands ( $10^011\leftarrow 00^001$ ,  $10^012\leftarrow 00001$ ,  $11^111\leftarrow 01101$ , and  $11^112\leftarrow 01^101$ ), for a total of 180 transitions. The claimed uncertainty for these data was in the order of 2%, at least for the two combination bands.

Ten years later, in 1998, Malathy Devi *et al.* [51], using a multispectrum non-linear least-squares fitting technique applied to absorption spectra recorded using the McMath-Pierce FTIR (at the National Solar Observatory, Kitt Peak), were capable of provide absolute line intensities for approximatively 1500  $^{16}\text{O}^{12}\text{C}^{16}\text{O}$  transitions, between 3090 and 3850  $\text{cm}^{-1}$ . The ultimate uncertainty of these experimental determinations strongly depended on the investigated transitions, ranging from 0.5 % for the strongest up to 30-40% for those belonging to the hot bands. Nevertheless, it must be pointed out that the authors of [51] claimed that some unexpected discrepancies were noticed between their results and those provided in Refs. [50, 41].

One of the most complete and comprehensive experimental work that has been performed in this spectral region (at least for the 626 isotopologue), can be considered the one done by André *et al.* in 2004 [52]. Here, the intensities (and the positions) of 453 transitions of twelve  $^{16}\text{O}^{12}\text{C}^{16}\text{O}$  rovibrational bands were determined, in the range 3700-3750  $\text{cm}^{-1}$ . Spectra were recorded by means of a FITR, at three different temperatures, namely 294, 500, and 698 K. The relative uncertainty on S did not exceed the 10%, being in most cases below the 5% level. For what concerns the two strong combination bands, this work provided data only for the  $10^011\leftarrow 00^001$  band. On the other hand, it is worth noting that the relative differences between these experimental data and the data provided at that time by HITRAN (HITRAN2000 version) were in most of the cases below the 5% (at least for the strongest transitions).

The most recent experimental line intensity data have been provided ten years ago by Jacquemart *et al.* [48]. With an experiment based on a Bruker FTIR, spectra were recorded in a very broad spectral region, from 2000 to 9000  $\text{cm}^{-1}$ . Among all the bands observed, the authors provided data also for those of the DP=5 polyad. In particular, they performed measurements for 52 and 53 transitions of the 626 isotopologue in the bands  $10^011\leftarrow 00^001$  and  $11^111\leftarrow 01^101$ , respectively. The absolute accuracy for these measurements was around 3%. Among the results obtained in this work, measurements were obtained for the first time for the  $10^011\leftarrow 00^001$  band of  $^{17}\text{O}^{12}\text{C}^{17}\text{O}$ ,  $^{16}\text{O}^{12}\text{C}^{17}\text{O}$ ,  $^{16}\text{O}^{12}\text{C}^{18}\text{O}$ , and  $^{18}\text{O}^{12}\text{C}^{18}\text{O}$  species, for the  $00^011\leftarrow 00^001$  band of  $^{17}\text{O}^{12}\text{C}^{18}\text{O}$ , and for the  $2001i\leftarrow 00001$  ( $i=1, 2$ , and  $3$ ) bands of the  $^{16}\text{O}^{12}\text{C}^{17}\text{O}$  isotopologue. It is worth noting

that for the  $10^011\leftarrow 00^001$  band significant deviations have been found as compared to the data provided in [50], while a good agreement, at least for transitions at the end of the R-branch, was observed with respect to Ref. [52].

In addition to the works discussed here above, there are only two examples of line strength measurements performed by means of diode laser spectroscopy. With respect to works based on FTIR, these studies were limited only to few transitions. Farooq *et al.* [53] have determined the line strength of the R(28) ( $10^012\leftarrow 00^001$  band) and P(70) ( $10^011\leftarrow 00^001$  band) transitions at 3633.08 and 3645.56  $\text{cm}^{-1}$ , respectively. These measurements were performed in a wide range of temperature (300-1000 K), being the overall uncertainty of their determinations about 2%.

On the other hand, in 2013, scientists from the Physikalisch-Technische Bundesanstalt (PTB) have published a very interesting paper based on the use of tuneable diode laser absorption spectroscopy (TDLAS) for line strength measurements [54]. This paper represents, to the best of our knowledge, the only experimental work in which a combination of direct TDLAS and metrological principles was employed for accurate determination of  $S$  (at this wavelength). An overall uncertainty of 0.5% (0.6%) was achieved in the determination of the line strength of the P36e (P34e) transition belonging to the  $10^011\leftarrow 00^001$  band. In both cases, the obtained  $S$ -values were in good agreement with those provided by HITRAN.

Here, it is worth mentioning also the work performed by R.A. Toth and coworkers at the Jet Propulsion Laboratory (JPL). In the late 2000s, using a FTIR spectrometer, the line strengths of more than 6000 transitions of the less abundant  $^{13}\text{C}$  and  $^{18}\text{O}$   $\text{CO}_2$  isotopologues were provided, along with a detailed comparison with the HITRAN data available at that time. These data were collected with uncertainty ranging from 1 to 20 % [55,47].

Finally, Table 5 summarizes the results of this section.

### 3.6 Line intensity of $\text{CO}_2$ near 2 $\mu\text{m}$

The  $\text{CO}_2$  Fermi triad consists of three  $\Sigma$ -symmetry bands,  $4\nu_2+\nu_3$  at 4853.6231  $\text{cm}^{-1}$ ,  $\nu_1+2\nu_2+\nu_3$  at 4977.8346  $\text{cm}^{-1}$  and  $2\nu_1+\nu_3$  at 5099.6601  $\text{cm}^{-1}$  ( $20^013\leftarrow 00^001$ ,  $20^012\leftarrow 00^001$  and  $20^011\leftarrow 00^001$  in the notation scheme used in the HITRAN database [5]). At room temperature the hot transitions  $21^11n\leftarrow 01^11$  ( $n = 1\dots 3$ ) are clearly visible. Table 6 lists several literature sources, reporting the line intensities of  $\text{CO}_2$  in the region of Fermi-triad. The newest edition of HITRAN database [5] states the uncertainty codes of intensities for the region of triad being 7 (1-2%) for  $20^011\leftarrow 00^001$ , and 8 (<1%) for  $20^012\leftarrow 00^001$  and  $20^013\leftarrow 00^001$ .  $20^011\leftarrow 00^001$  is the least studied because of its proximity to the absorption of organic molecules (such as methane [56]) and the combination band of water [57]).

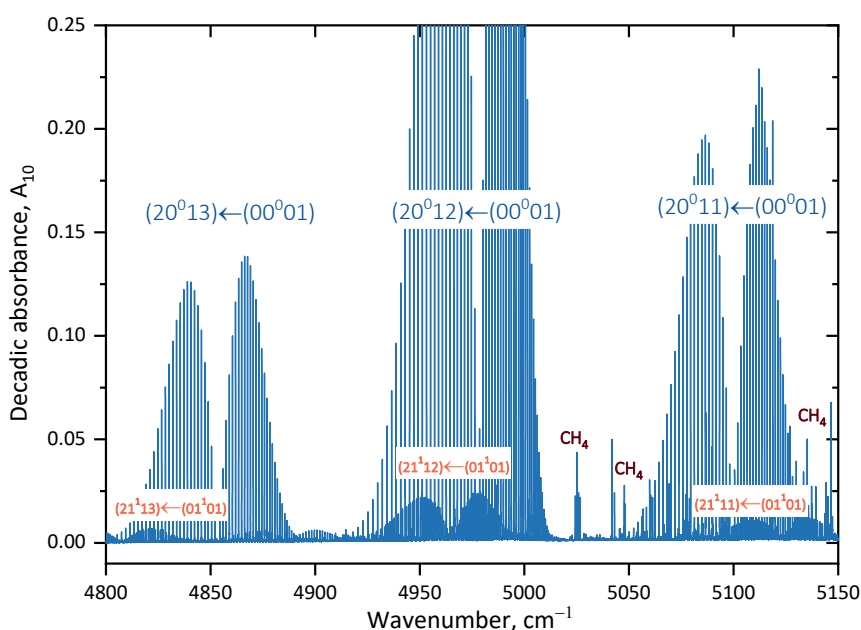


**Figure 0-1.** Overview of the  $\text{CO}_2$  triad. Spectrum was measured 0.005  $\text{cm}^{-1}$  nominal resolution with 3.5 m pathlength. The sample was a mixture of 5 hPa  $\text{CO}_2$  with c.a. 100 hPa of methane. Source: Ref. [56].

The triad became a scope of interest in the 90-es. Several experimental works, involving different laser-based techniques [58, 59, 60, 61, 62, 63] were focusing on it. They report intensities for a small sets of lines, sometimes even only one line as in refs. 58, 61 and 62.

Works by Michalcea et al. [58], Webber et al. [61] and Geng et al. [60] are of a special interest for the current project. In Ref. [58] the intensity of R<sub>56</sub> line in 20<sup>0</sup>12←00<sup>0</sup>01 band is measured in a very large span of elevated temperatures, from 300 to 1425 K. The study by Webber [61] reports the intensity measurement of R<sub>50</sub> line of the same band and it use for the concentration monitoring at combustion regime (1500 K). Another article [60] reports intensities of three lines in the middle band at low temperatures, down to 110 K.

Whereas the laser-based experimental works are focused solely on the main isotopologue, the broadband studies by R. Toth, M. Devi, K. Benner and coworkers [55,47,64] report a large set of different isotopologues and all components of the triad. The cumulative work by the same authors [64] is of particular importance. The FT-spectra of neat CO<sub>2</sub> and its mixtures with air at different pressures, temperatures, pathlength and with different isotopic compositions (<sup>12</sup>C and <sup>13</sup>C) recorded in that study were used as an input for a multispectrum non-linear least squares curve fitting technique. Very extensive and accurate set of various spectral line parameters are reported, setting a current standard for CO<sub>2</sub> in this region. One should note that although the uncertainties resulting from the fit itself are small (0.045% for intensities), overall uncertainties remain at about 0.5% due to systematic contributions from absorption paths, temperature measurements etc. the level of a few percent to a sub-percent level is typical (and expected) from the broadband measurements with incoherent sources.

Table 6. Summary of the experimental works reporting the intensity data for the triad of CO<sub>2</sub> (2 μm). Relative uncertainties of line strengths are a standard deviation (k=1).

Ref.	Year	Technique	Bands	Number of transitions	Iso.	ΔS/S, %
[58]	1998	TDLAS	20 <sup>0</sup> 12←00 <sup>0</sup> 01	R <sub>56</sub>	626	Not specified
[59]	1999	DFB-laser	20 <sup>0</sup> 12←00 <sup>0</sup> 01	13: R <sub>22</sub> -R <sub>46</sub>	626	3-4%
[60]	2001	ILS technique	20 <sup>0</sup> 12←00 <sup>0</sup> 01	3: (P <sub>12</sub> , P <sub>14</sub> , P <sub>16</sub> )	626	Not specified
[61]	2001	TDLAS	20 <sup>0</sup> 12←00 <sup>0</sup> 01	1: R <sub>50</sub>	626	3%
[62]	2004	TDLAS	20 <sup>0</sup> 13←0 <sup>0</sup> 001	1: R <sub>26</sub>	626	3%
[63]	2005	TDLAS	20 <sup>0</sup> 12←00 <sup>0</sup> 01	5 7	636 638	2-4% for <sup>13</sup> C 3% for <sup>18</sup> O
[64] [55, 47]***	2006	FTIR	20 <sup>0</sup> 13←0 <sup>0</sup> 001 20 <sup>0</sup> 12←00 <sup>0</sup> 01 20 <sup>0</sup> 11←00 <sup>0</sup> 01	68 51 70	626	0.58%* 0.44% 0.62%
[65]	2006	FTIR/TDLAS	20 <sup>0</sup> 13←0 <sup>0</sup> 001 20 <sup>0</sup> 12←00 <sup>0</sup> 01	43 45	626	10%** 3%**
[66]	2008	TDLAS	20 <sup>0</sup> 13←0 <sup>0</sup> 001	3	626	1-0.3%
[67]	2016	FTIR	20 <sup>0</sup> 13←0 <sup>0</sup> 001	1514	626	0.045% fit 0.5% systematic
[68]	2020	CRD	20 <sup>0</sup> 13←0 <sup>0</sup> 001	39	626	0.07% type B uncertainty

\* Standard deviation between observed and computed line strengths.

\*\* difference with HITRAN 2000

\*\*\* References [55] and [47] are follow-up studies, reporting line data for several isotopologues and the dyad as well. See section “Line intensity of CO<sub>2</sub> at 2.8 μm”.

Another important work is a recent study by H. Fleurbaey et al. [68]. It is a broadband study with (39 lines were recorded and analysed), but the method was not a conventional FT-IR but CRD-based. The authors performed a meticulous uncertainty analysis, yielding impressive 0.08% uncertainty for the integrated intensity for



$20^013 \leftarrow 00^001$  band of the major isotopologue. The authors of [68] also report systematic deviations between their intensities and the literature data.

Broadening and shifting coefficients are of interest for current project, since they determine the spectral line shapes and depend on temperature. Analysis of the shifts or broadening can provide an additional cross-check to the temperatures, obtained from the intensity analysis. In this field PTB team together with WP1 leader A. Kiuberis have accumulated substantial experience with the measurement and analysis collisional parameters of Fermi triad at room temperature, which resulted in a mutual paper [56]. Uncertainties of the broadening and shifting coefficients in this work are in a typical interval of 0.3 % and 2-3% respectively ( $k = 1$ ).

Ref. [69], focused on comparison of the collisional spectral parameters, namely shifting, broadening as well as their temperature dependence, provides an excellent literature overview prior 2014. More recent works are citing [69] and can easily be found.

Ref. [69] reports significant inconsistencies and systematic deviations among the values from different experimental studies. The authors come to a similar conclusion as in [69]: “the multi spectrum technique can determine spectrum line half-widths with an uncertainty better than 0.1%, but the systematic uncertainties have always limited the absolute accuracy of half-widths determined from experimental spectra to 1–2%”. It is likely that the reported uncertainties often underestimated the actual uncertainties because systematic contributions to measurement uncertainty are not considered. In the future, researchers should report the true error of the measurements.” These observations make it necessary to revise existing knowledge and make new measurements with a specific target of uncertainty analysis which is one of the goals of PriSpecTemp.

### 3.7 Line intensity of CO<sub>2</sub> at 1.60 μm and 1.57 μm

Line parameters in HITRAN2020 [5] for both  $30^013 \leftarrow 00^001$  band ( $6230 \text{ cm}^{-1}$ ,  $1.6 \mu\text{m}$ ) and  $30^012 \leftarrow 00^001$  band ( $6350 \text{ cm}^{-1}$ ,  $1.57 \mu\text{m}$ ) are adopted from the same set of references. Line positions are from Ref. [32] with uncertainties  $\geq 0.001$  and  $< 0.01 \text{ cm}^{-1}$ . Line intensities are referenced to Ref. [70] and have estimated uncertainties below 1% (code 8). The original source of line intensities for  $30^013$  and  $30^012$  bands that serve for an update of HITRAN is Ref. [71] from NIST. They were measured with frequency-comb referenced cavity ring-down spectroscopy with a signal-to-noise level of spectra between  $5 \times 10^3$  and  $5 \times 10^4$  and reported relative combined standard uncertainties below 0.1%. Fig. 1 in Ref. [71] shows comparison of these line intensities with other databases. Differences between datasets are of the order of percent or more for individual lines, and they exhibit not only an offset but also J-dependence. Only for  $30^013$  band data agree better than within 0.5% between experimental [71] and ab initio [72] with permille-level agreement on average.

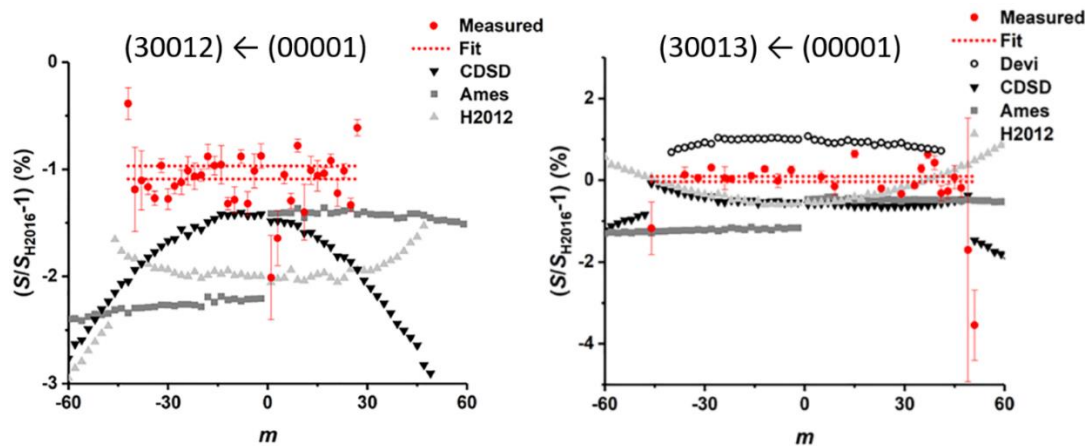


**Figure 0-2.** Relative  $^{12}\text{C}^{16}\text{O}_2$  line intensity differences between HITRAN 2016 [1] (based on ab initio calculations [72]) and other available datasets: “Measured” [71], “Devi” [78], CDSD [31], Ames [73]), HITRAN 2012 [74]. Adopted from Fig. 1 of Ref. [71].

High-accuracy line parameters for both  $30^013$  and  $30^012$  bands were provided in Ref. [75]. They were measured with a Fourier-transform spectrometer at DLR. Line positions, self-shifts, intensities, self-broadenings, their quadratic speed dependence, and the first-order line mixing were provided. The reported combined systematic standard uncertainty of line intensities was 0.15%. The relative differences between line intensities of [75] and [71] are shown in Fig. 2. For  $30^013$  and  $30^012$  bands the averaged differences are -0.233% and -0.521%, respectively. The latter one is more than three times the reported combined standard uncertainty. On the other hand, there is nearly the same ratio of [75]-to-[76] line intensities for  $30^013$  and  $30^012$  bands equal 1.0041.

The line intensities in the ABSCO 5.1 database [77] for the 30<sup>0</sup>13 band are data from Ref. [78] rescaled by 1.4% and they are 0.4%-0.9% larger than DLR intensities. These differences are systematic with rotational quantum number J – they increase with J as shown in Fig. 18 of Ref. [75]. On the other hand, NIST and DLR data there is no clear trend of the intensity ratios with J.

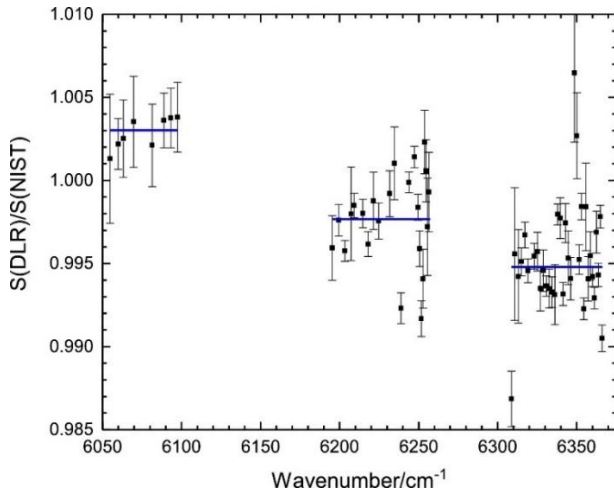


**Figure 0-3.** Ratios of DLR [75] to NIST [71] line intensities and their weighted averages for CO<sub>2</sub> bands 30<sup>0</sup>14, 30<sup>0</sup>13, and 30<sup>0</sup>12. Adopted from Fig. 17 of Ref. [75].

Ab initio dipole moment surface reported in Ames-2021 [79] provides CO<sub>2</sub> line intensities with a few permille level agreement with NIST and DLR results. This comparison is shown in Fig. 3 (adopted from Fig. 4 of Ref. [79]). The mean relative differences between NIST and Ames are 0.2 ‰ for (30<sup>0</sup>12) and 2.39 ‰ for (30<sup>0</sup>13) bands and corresponding differences between DLR and Ames are -5.03 ‰ and 0.5 ‰.

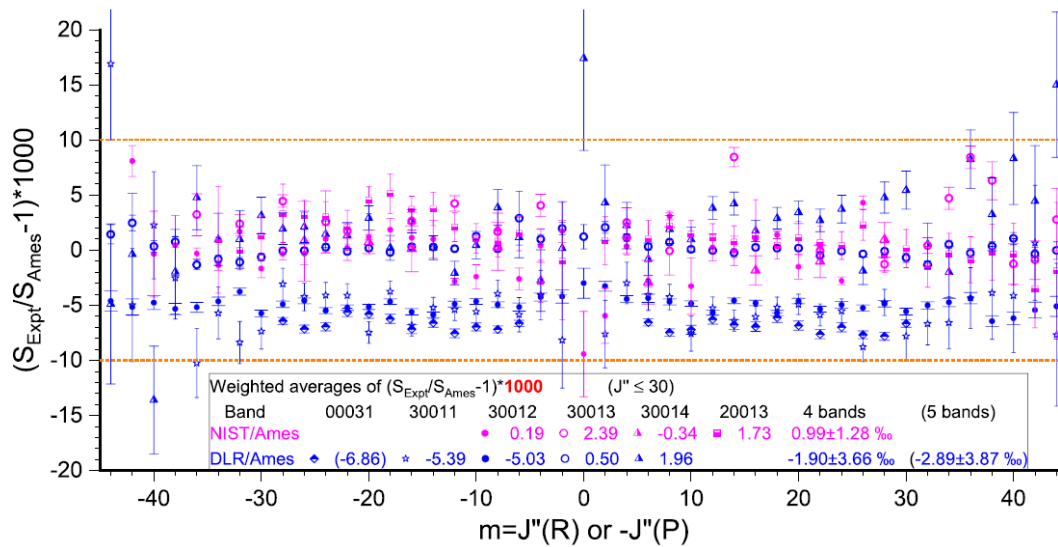


**Figure 0-4.** Relative differences between experimental ( NIST [71] and DLR [75]) and theoretical Ames-2021 [79] line intensities of <sup>12</sup>C<sup>16</sup>O<sub>2</sub> for different IR bands. Adopted from Fig. 4 of Ref. [79].

The line-shape parameters are available for the Voigt and quadratic speed-dependent Voigt profiles. The line-mixing parameters Y are also available together with its temperature-dependence exponent. Most of the air-broadened and some self-broadened parameters ( $\gamma_{\text{air}}$ ,  $n_{\text{air}}$ ,  $n_{\text{self}}$ ,  $\gamma_{\text{self}}$ ,  $\gamma_{\text{air}}$ ,  $\gamma_{\text{SDV}_0\text{air}_{296}}$ ,  $n_{\text{SDV}_{\text{air}_{296}}}$ ,  $\gamma_{\text{SDV}_2\text{air}_{296}}$ ,  $\delta_{\text{SDV}_0\text{air}_{296}}$ ,  $n_{\text{SDV}_{\text{self}_{296}}}$ ,  $\delta_{\text{SDV}_0\text{self}_{296}}$ ,  $\gamma_{\text{SDV}_{\text{air}_{296}}}$ ,  $\gamma_{\text{SDV}_{\text{self}_{296}}}$ ,  $n_{\gamma_{\text{SDV}_2\text{air}_{296}}}$ ,  $n_{\gamma_{\text{SDV}_{\text{air}_{296}}}}$ ) are estimated as explained in Ref. [80]. In Ref. [80], the air- and self-broadening and their temperature dependencies were evaluated based on available experimental data. The pressure shift parameters were calculated with a semi-empirical approach based on available experimental data. These line-shape parameters were used for calculating the first-order line-mixing. The remaining self-broadening parameters are:  $\gamma_{\text{self}}$  from Pade approximation to the data available in [81, 82, 75, 80] as described in Ref. [83],  $\delta_{\text{air}}$  from Ref. [84],  $\delta_{\text{self}}$ ,  $\gamma_{\text{SDV}_0\text{self}_{296}}$ ,  $\gamma_{\text{SDV}_2\text{self}_{296}}$  from Ref. [75]. Comparison of self-broadening and shifting between [75], [80] and [78] is shown in [75]. The broadening  $\gamma_{0\text{self}}$  agree within 1% - 2%, and the speed-dependent broadening  $\gamma_{2\text{self}}$  differ by up to 30% - 40% between these three sources.



## 4 Oxygen, O<sub>2</sub>

### 4.1 A-band of O<sub>2</sub> (0.76 μm)

The A-band of molecular oxygen (O<sub>2</sub>) is one of the bands arising from the  $b^1\Sigma_g^+ \leftarrow X^3\Sigma_g^-$  electronic transition. The transition is electric dipole and spin forbidden, but magnetic dipole allowed. For the A-band, the vibrational state remains unchanged, leading to an absorption band centered at 762 nm (13 122 cm<sup>-1</sup>), see Figure 4-1. The practical importance of the oxygen A-band stems from the needs of atmospheric remote sensing. Owing to its well-known and uniform mixing ratio over the full range of atmospheric conditions, O<sub>2</sub> is used to calibrate intensities of atmospheric spectra taken by satellite and ground-based instruments [85]. The A-band is particularly important because it is largely free of spectral interferences from other atmospheric species, and many of the A-band transitions are relatively weak and do not saturate for long pathlengths [86]. The stringent precision requirements of CO<sub>2</sub> monitoring have motivated the work towards ever-more accurate O<sub>2</sub> A-band intensity measurements [85,87].

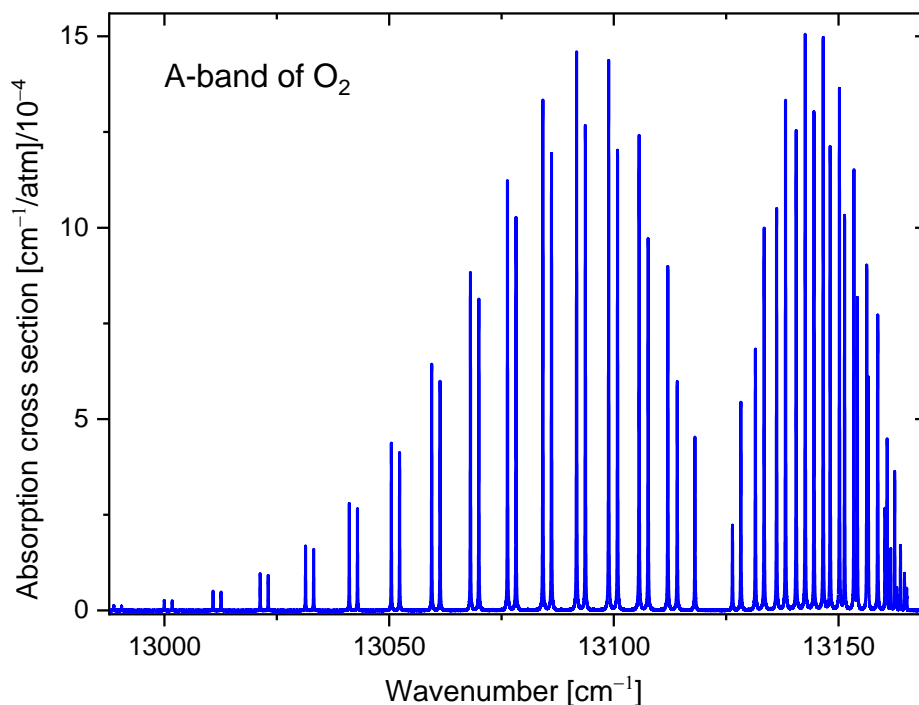


Figure 4-1. Overview of the absorption spectrum of oxygen in the A-band (measured at PTB).

The rotational energy levels of molecular oxygen are described by the quantum numbers  $J$  and  $N$ , where  $N$  is the rotational angular momentum and  $J$  is the total angular momentum:  $J = N + S$ , with  $S$  denoting the spin angular momentum. The triplet ( $S = 1$ ) ground state has rotational levels  $J'' = N'', N'' \pm 1$ , while the excited electronic state  $b$  is a singlet state ( $S = 0$ ) with rotational levels  $J' = N'$ . As a result, four types of transitions (branches) appear, labeled  $\Delta N \Delta J$ :  $PP$ ,  $PQ$ ,  $RQ$  and  $RR$ , where  $P$ ,  $Q$ , and  $R$  denote angular momentum quantum number changes of  $-1$ ,  $0$ , and  $+1$ , respectively. Transitions  $PP(N'', J'' = N'' + 1)$  and  $PQ(N'', J'' = N'' - 1)$  form the  $P$  branch with about 2 cm<sup>-1</sup> line separation. Transitions  $RR$  and  $RQ$  form the  $R$  branch with a decreasing line separation for higher  $J$ , leading to a bandhead at about 13 156 cm<sup>-1</sup>.

Individual transitions are labeled  $\Delta N N'' \Delta J J''$ . For example, P7Q6 denotes a transition that starts from state  $N'' = 7$ ,  $J'' = 6$  and for which the angular momentum changes are  $\Delta N = -1$ ,  $\Delta J = 0$ . Angular momentum index  $m$  is often used when plotting the line intensities as a function of the initial state – as an example, see Figure 4-2. For the  $PP$  and  $PQ$  branches the index is defined  $m = -J''$  and for the  $RR$  and  $RQ$  branches it is  $m = J'' + 1$  [86].

Key papers reporting O<sub>2</sub> A-band line intensities and other parameters are listed in Table 7. Significantly reduced uncertainties of the line intensities have been obtained after the HITRAN 2008 update. The most recent (2008 onwards) experimental data are largely from the frequency-stabilized cavity ring-down spectroscopy (FS-CRDS) measurements of the Hodges group (NIST) [88,89,86,90]. The first FS-CRDS measurements focused on the  $P$  branch [88,90], including rare O<sub>2</sub> isotopologues [89]. In 2010-2011 the group extended their study to the  $R$  branch, measuring several lines of not only the main isotopologue [86] but also of rare isotopologues [91]. Some of the newer line lists include Dicke narrowing parameters, which allow for

calculation of the Galatry line profile and corrected a calculation error in the HITRAN database which led the O<sub>2</sub> line intensities to have an incorrect frequency dependence [92].

Recent contributions have highlighted the importance of collision-induced absorption (CIA) and line mixing effects, with an effort to upgrade the Absorption coefficient (ABSCO) look-up tables used for Orbiting Carbon Observatory (OCO) missions [85,87,77]. These effects have been better characterized via measurements at higher pressures and by applying new multispectrum fitting software with sophisticated line-shape models such as Rautian and speed-dependent Voigt; see Drouin *et al.* [85], which also includes discussion about Galatry vs. speed-dependent line shape models and mentions ongoing efforts on applying Hartmann-Tran profile. Detailed comparisons of different line shape models (Galatry, speed-dependent Voigt & Rautian) can also be found in the paper of Predoi-Cross *et al.*, which reports line intensities and other parameters obtained from multispectrum fits of high-resolution FTS measurements [93].

The 2020 contribution of Payne *et al.* combines earlier FS-CRDS measurements with new FT-CRDS and Fourier Transform Spectroscopy (FTS) measurements [77]. These have been included to provide full band coverage and more comprehensive information at various temperatures and pressures. It is worth pointing out the discussion in section 2.3.2. which states “*The inspection revealed and overlooked inconsistency between the FTRS and CRDS in prior work of several percent, as well as a similar inconsistency between the ‘new’ [77] CRDS and the prior CRDS data in this same region...*” thus suggesting that there is need for further scrutiny of the oxygen A-band line intensities, the P-branch in particular. Nevertheless, the article [77] nicely summarizes the status of oxygen spectroscopy in the context of Orbiting Carbon Observatories and is given as the main reference in HITRAN 2020 for the data of oxygen A-band.

As for the HITRAN 2020 update [1], oxygen A-band line intensities were “*changed up to 5% at higher J values due to a re-assessment of the high-J data [88] to determine Herman-Wallis terms utilized in the last two HITRAN editions [86]*”; see Figure 4-2.

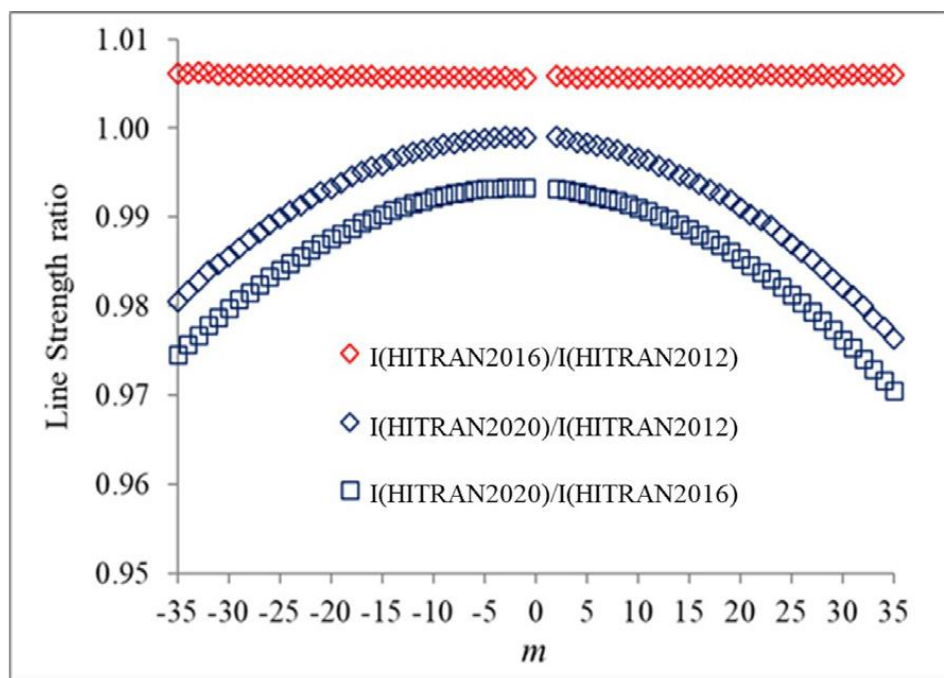


Figure 4-2. Ratios of intensities from HITRAN 2020 (ABSCO 5.1) [77] compared with HITRAN 2016 [1] and HITRAN 2012 [74]. The HITRAN 2016 update, which utilized a prior ABSCO release (5.0) kept the Herman-Wallis factors from HITRAN 2012 fixed. The changes are due to band scaling and the application of new Herman-Wallis factors.

Weaker O<sub>2</sub> absorption lines that overlap with the magnetic dipole A-band include the A-band electric quadrupole transitions [94] and the (magnetic dipole) hot band  $\nu' = 1 \leftarrow \nu'' = 1$  [95]. Although the electric quadrupole transitions are about  $10^5$  times weaker than the respective magnetic dipole allowed transitions, they can be observed in atmospheric spectra with up to 1 % absorbance. Some of the strongest electric quadrupole transitions (with line intensities of about  $10^{-29}$  cm molec<sup>-1</sup>) have been measured with FS-CRDS [94]. As for the hot band, the line intensities are in room temperature about three orders of magnitude weaker than those of the A-band; several lines have nevertheless been measured [95].

Table 7. Summary of the experimental works reporting the intensity data for the A-band of O<sub>2</sub>. Uncertainties and accuracies reflect the relative quality of the datasets. For a detailed information about uncertainty evaluation, one should address original sources.

Ref.	Published	Technique	Number of transitions	Isotopologues	Notes on the measured line intensity
[96]	1987	TDLAS	54	<sup>16</sup> O <sub>2</sub>	~1% variation in linestrengths determined in different pressures
[97]	1999	FTS+LPAC	Not specified	<sup>16</sup> O <sup>18</sup> O	Accuracy: 10%
[98]	1999	FTS+LPAC	Not specified	<sup>16</sup> O <sub>2</sub>	Accuracy: 0.3%
[99]	2000	FTS	44	<sup>16</sup> O <sub>2</sub>	Measurement precision: 1% Absolute accuracy 2%
[95]	2004	NICE-OHMS	12 ( <sup>16</sup> O <sub>2</sub> ), 17 ( <sup>16</sup> O <sup>18</sup> O)	<sup>16</sup> O <sub>2</sub> <sup>16</sup> O <sup>18</sup> O	Experimental precision: Stronger lines: ~10% Weaker lines: errors ~90%
[100]	2007	TDLAS	~40	<sup>16</sup> O <sub>2</sub>	Average uncertainty: ±3% Deviation from the database: -8%
[93]	2008	FTS	56	<sup>16</sup> O <sub>2</sub>	Accuracy: ~1%
[88]	2008	FS-CRDS	32	<sup>16</sup> O <sub>2</sub>	~1% lower results than in the databases
[89]	2009	FS-CRDS	65 ( <sup>16</sup> O <sup>18</sup> O), 54 ( <sup>16</sup> O <sup>17</sup> O)	<sup>16</sup> O <sup>17</sup> O, <sup>16</sup> O <sup>18</sup> O, <sup>17</sup> O <sup>18</sup> O, <sup>18</sup> O <sub>2</sub>	<sup>16</sup> O <sup>18</sup> O: ~2% deviation of the database values, <sup>16</sup> O <sup>17</sup> O: systematic offset compared to database
[90]	2009	FS-CRDS	20	<sup>16</sup> O <sub>2</sub>	High J-transitions
[86]	2010	FS-CRDS	34(R-branch)	<sup>16</sup> O <sub>2</sub>	Relative st. dev. 0.3%
[91]	2011	FS-CRDS	100 (R-branch)	<sup>16</sup> O <sup>17</sup> O, <sup>16</sup> O <sup>18</sup> O, <sup>17</sup> O <sub>2</sub> , <sup>17</sup> O <sup>18</sup> O, <sup>18</sup> O <sub>2</sub>	
[85]	2017	FS-CRDS, FTS	Not specified	<sup>16</sup> O <sub>2</sub>	

## 5 References

- <sup>1</sup> I.E. Gordon, L.S. Rothman, C. Hill, R.V. Kochanov, Y. Tan, P.F. Bernath, M. Birk, V. Boudon, A. Campargue, K.V. Chance, B.J. Drouin, J.-M. Flaud, R.R. Gamache, J.T. Hodges, D. Jacquemart, V.I. Perevalov, A. Perrin, K.P. Shine, M.-A.H. Smith, J. Tennyson, G.C. Toon, H. Tran, V.G. Tyuterev, A. Barbe, A.G. Császár, V.M. Devi, T. Furtenbacher, J.J. Harrison, J.-M. Hartmann, A. Jolly, T.J. Johnson, T. Karman, I. Kleiner, A.A. Kyuberis, J. Loos, O.M. Lyulin, S.T. Massie, S.N. Mikhailenko, N. Moazzen-Ahmadi, H.S.P. Müller, O.V. Naumenko, A.V. Nikitin, O.L. Polyansky, M. Rey, M. Rotger, S.W. Sharpe, K. Sung, E. Starikova, S.A. Tashkun, J. Vander Auwera, G. Wagner, J. Wilzewski, P. Wcisło, S. Yu, E.J. Zak, The HITRAN2016 molecular spectroscopic database, *JQSRT* **203**, 3-69 (2017). Doi: [10.1016/j.jqsrt.2017.06.038](https://doi.org/10.1016/j.jqsrt.2017.06.038).
- <sup>2</sup> G.Li, I. E. Gordon, L. S. Rothman, Y. Tan, S.-M. Hu, S. Kassi, A. Campargue, and E. S. Medvedev Rovibrational line lists for nine isotopologues of the CO molecule in the  $X^1\Sigma^+$  ground electronic state. The *Astrophysical Journal Supplement Series*, **216**(1), 15 (2015). DOI [10.1088/0067-0049/216/1/15](https://doi.org/10.1088/0067-0049/216/1/15).
- <sup>3</sup> Y. Tan, J. Wang, X.-Q. Zhao, A.-W. Liu, S.-M. Hu, Cavity ring-down spectroscopy of the fifth overtone of CO, *JQSRT* **187**, 274-279 (2017) Doi: [10.1016/j.jqsrt.2016.10.003](https://doi.org/10.1016/j.jqsrt.2016.10.003).
- <sup>4</sup> J.A. Coxon, P.G. Hajigeorgiou. Direct potential fit analysis of the  $X^1\Sigma^+$  ground state of CO. *J. Chem. Phys.*, **121**, 2992-3008 (2004). Doi: [10.1063/1.1768167](https://doi.org/10.1063/1.1768167)
- <sup>5</sup> Gordon, I.E., Rothman, L.S., Hargreaves, R.J., Hashemi, R., Karlovets, E.V., Skinner, F.M., Conway, E.K., Hill, C., Kochanov, R.V., Tan, Y., Wcisło, P., Finenko, A.A., Nelson, K., Bernath, P.F., Birk, M., Boudon, V., Campargue, A., Chance, K.V., Coustenis, A., Drouin, B.J., Flaud, J. –M., Gamache, R.R., Hodges, J.T., Jacquemart, D., Mlawer, E.J., Nikitin, A.V., Perevalov, V.I., Rotger, M., Tennyson, J., Toon, G.C., Tran, H., Tyuterev, V.G., Adkins, E.M., Baker, A., Barbe, A., Canè, E., Császár, A.G., Dudaryonok, A., Egorov, O., Fleisher, A.J., Fleurbaey, H., Foltynowicz, A., Furtenbacher, T., Harrison, J.J., Hartmann, J. –M., Horneman, V. –M., Huang, X., Karman, T., Karns, J., Kassi, S., Kleiner, I., Kofman, V., Kwabia-Tchana, F., Lavrentieva, N.N., Lee, T.J., Long, D.A., Lukashetskaya, A.A., Lyulin, O.M., Makhnev, V.Y., Matt, W., Massie, S.T., Melosso, M., Mikhailenko, S.N., Mondelain, D., Müller, H.S.P., Naumenko, O.V., Perrin, A., Polyansky, O.L., Raddaoui, E., Raston, P.L., Reed, Z.D., Rey, M., Richard, C., Tóbiás, R., Sadiek, I., Schwenke, D.W., Starikova, E., Sung, K., Tamassia, F., Tashkun, S.A., Auwera, J. Vander, Vasilenko, I.A., Vigasin, A.A., Villanueva, G.L., Vispoel, B., Wagner, G., Yachmenev, A., Yurchenko, S.N. The HITRAN2020 molecular spectroscopic database. *JQSRT* **277**, 107949 (2022). Doi: [10.1016/j.jqsrt.2021.107949](https://doi.org/10.1016/j.jqsrt.2021.107949)
- <sup>6</sup> R. Hashemi, I. E. Gordon, E.M. Adkins, J. T. Hodges, D. A. Long, M.Birk, J. Loos, C. D. Boone, A. J. Fleisher, A. Predoi-Cross, L. S. Rothman, Improvement of the spectroscopic parameters of the air- and self-broadened  $N_2O$  and CO lines for the HITRAN2020 database applications, *JQSRT* **271**, 107735 (2021). Doi: [10.1016/j.jqsrt.2021.107735](https://doi.org/10.1016/j.jqsrt.2021.107735).
- <sup>7</sup> M. V. Devi, C.D. Benner, K. Sung, T. J. Crawford, G. Li, R. R. Gamache, M.A.H. Smith, I. E. Gordon, A. W. Mantz, Positions, intensities and line shape parameters for the  $1\leftarrow 0$  bands of CO isotopologues, *JQSRT* **218**, 203-230 (2018). Doi: [10.1016/j.jqsrt.2018.06.007](https://doi.org/10.1016/j.jqsrt.2018.06.007).
- <sup>8</sup> A. Cygan, P. Wcisło, S. Wójtewicz, G. Kowzan, M. Zaborowski, D. Charczun, K. Bielska, R. Trawiński, R. Ciuryło, P. Masłowski, and D. Lisak, "High-accuracy and wide dynamic range frequency-based dispersion spectroscopy in an optical cavity," *Opt. Express* **27**, 21810-21821 (2019). Doi: [10.1364/OE.27.021810](https://doi.org/10.1364/OE.27.021810)
- <sup>9</sup> L.S. Rothman, I.E. Gordon, R.J. Barber, H. Dothe, R.R. Gamache, A. Goldman, et al. HITRAN, the high-temperature molecular spectroscopic database. *JQSRT* **111** 2139-50 (2010). Doi: [10.1016/j.jqsrt.2010.05.001](https://doi.org/10.1016/j.jqsrt.2010.05.001)
- <sup>10</sup> D. Goorvitch, Infrared CO Line List for the  $X^1\Sigma^+$  State. *Astrophys. J. Suppl. Series*, **95**, 535 (1994). doi: [10.1086/192110](https://doi.org/10.1086/192110).
- <sup>11</sup> D. Goorvitch, C. Chackerian, Rovibrational Intensities of the Minor Isotopes of the CO  $X^1\Sigma^+$  State for  $v \leq 20$  and  $J \leq 150$ , . *Astrophys. J. Suppl. Series* **92**, 311 (1994). Doi: [10.1086/191970](https://doi.org/10.1086/191970).
- <sup>12</sup> Holger S.P. Müller, F. Schlöder, J. Stutzki, G. Winnewisser, The Cologne Database for Molecular Spectroscopy, CDMS: a useful tool for astronomers and spectroscopists, *J. Mol. Struct.*, **742**(1–3), 215-227 (2005). Doi: [10.1016/j.molstruc.2005.01.027](https://doi.org/10.1016/j.molstruc.2005.01.027).

- <sup>13</sup> J.W Brault, L.R Brown, C. Chackerian, R. Freedman, A. Predoi-Cross, A.S. Pine, Self-broadened  $^{12}\text{C}^{16}\text{O}$  line shapes in the  $v=2 \leftarrow 0$  band, *J. Molecular Spectroscopy*, **222**(2), 220-239 (2003). Doi: [10.1016/j.jms.2003.07.002](https://doi.org/10.1016/j.jms.2003.07.002)
- <sup>14</sup> K. Sung, P. Varanasi, Intensities, collision-broadened half-widths, and collision-induced line shifts in the second overtone band of  $^{12}\text{C}^{16}\text{O}$ , *JQSRT*, **83**(3–4), 445-458 (2004). Doi: [10.1016/S0022-4073\(03\)00015-3](https://doi.org/10.1016/S0022-4073(03)00015-3)
- <sup>15</sup> V. V. Meshkov, E. A. Pazyuk, Stolyarov, A. V. A robust dipole moment of carbon monoxide (CO) is a permanent puzzle for both spectroscopic and *ab initio* studies. *Molecular Physics*. (2024) Doi: [10.1080/00268976.2024.2429740](https://doi.org/10.1080/00268976.2024.2429740) (article ASAP on 13.01.2025).
- <sup>16</sup> A. A. Balashov, K. Bielska, G. Li, A. A. Kyuberis, S. Wójtewicz, J. Domysławska, R. Ciuryło, N. F. Zobov, D. Lisak, J. Tennyson, O. L. Polyansky; Measurement and calculation of CO ( $7 \leftarrow 0$ ) overtone line intensities. *J. Chem. Phys.* **21**, 158 (2023): 234306. Doi: [10.1063/5.0152996](https://doi.org/10.1063/5.0152996)
- <sup>17</sup> V.V. Meshkov, A.V. Stolyarov, A.Yu. Ermilov, E.S. Medvedev, V.G. Ushakov, I.E. Gordon, Semi-empirical ground-state potential of carbon monoxide with physical behavior in the limits of small and large inter-atomic separations, *JQSRT* **217**, 262-273 (2018). Doi: [10.1016/j.jqsrt.2018.06.001](https://doi.org/10.1016/j.jqsrt.2018.06.001)
- <sup>18</sup> V.V. Meshkov, A.Yu. Ermilov, A.V. Stolyarov, E.S. Medvedev, V.G. Ushakov, I.E. Gordon, Semi-empirical dipole moment of carbon monoxide and line lists for all its isotopologues revisited, *JQSRT* **280**, 108090 (2022). Doi: [10.1016/j.jqsrt.2022.108090](https://doi.org/10.1016/j.jqsrt.2022.108090)
- <sup>19</sup> Q. Zou, P. Varanasi, New laboratory data on the spectral line parameters in the  $1 \leftarrow 0$  and  $2 \leftarrow 0$  bands of  $^{12}\text{C}^{16}\text{O}$  relevant to atmospheric remote sensing, *JQSRT* **75**(1), 63-92 (2002). Doi: [10.1016/S0022-4073\(02\)00007-9](https://doi.org/10.1016/S0022-4073(02)00007-9)
- <sup>20</sup> J. Vanderover, M.A. Oehlschlaeger, A mid-infrared scanned-wavelength laser absorption sensor for carbon monoxide and temperature measurements from 900 to 4000 K. *Appl. Phys. B* **99**, 353–362 (2010). Doi: [10.1007/s00340-009-3849-5](https://doi.org/10.1007/s00340-009-3849-5)
- <sup>21</sup> A. Predoi-Cross, K. Esteki, H. Rozario, H. Naseri, S. Latif, F. Thibault, V. Malathy Devi, M.A.H. Smith, A.W. Mantz, Theoretical and revisited experimentally retrieved He-broadened line parameters of carbon monoxide in the fundamental band, *JQSRT* **184**, 322-340 (2016). Doi: [10.1016/j.jqsrt.2016.08.007](https://doi.org/10.1016/j.jqsrt.2016.08.007)
- <sup>22</sup> C.M. Grégoire, O. Mathieu, E.L. Petersen, High-temperature line strengths with He- and Ar-broadening coefficients of the P(20) line in the  $1\ 0$  band of carbon monoxide. *Appl. Phys. B* **129**, 187 (2023). Doi: [10.1007/s00340-023-08132-6](https://doi.org/10.1007/s00340-023-08132-6)
- <sup>23</sup> M. V. Devi, C. D. Benner, M.A.H. Smith, A.W. Mantz, K. Sung, L.R. Brown, A. Predoi-Cross, Spectral line parameters including temperature dependences of self- and air-broadening in the  $2 \leftarrow 0$  band of CO at  $2.3\ \mu\text{m}$ , *JQSRT* **113**(11), 1013-1033 (2012), Doi: [10.1016/j.jqsrt.2012.02.010](https://doi.org/10.1016/j.jqsrt.2012.02.010)
- <sup>24</sup> K. Esteki, A. Predoi-Cross, C. Povey, S. Ivanov, A. Ghoufi, F. Thibault, M.A.H. Smith, Room temperature self- and H<sub>2</sub>-broadened line parameters of carbon monoxide in the first overtone band: Theoretical and revised experimental results, *JQSRT* **203**, 309-324 (2017). Doi: [10.1016/j.jqsrt.2017.04.008](https://doi.org/10.1016/j.jqsrt.2017.04.008)
- <sup>25</sup> N. Jacquinet-Husson, R. Armante, N.A. Scott, A. Chédin, L. Crépeau, C. Boutammine, A. Bouhdaoui, C. Crevoisier, V. Capelle, C. Boone, N. Poulet-Crovisier, A. Barbe, D. Chris Benner, V. Boudon, L.R. Brown, J. Buldyreva, A. Campargue, L.H. Coudert, V.M. Devi, M.J. Down, B.J. Drouin, A. Fayt, C. Fittschen, J.-M. Flaud, R.R. Gamache, J.J. Harrison, C. Hill, Ø. Hodnebrog, S.-M. Hu, D. Jacquemart, A. Jolly, E. Jiménez, N.N. Lavrentieva, A.-W. Liu, L. Lodi, O.M. Lyulin, S.T. Massie, S. Mikhailenko, H.S.P. Müller, O.V. Naumenko, A. Nikitin, C.J. Nielsen, J. Orphal, V.I. Perevalov, A. Perrin, E. Polovtseva, A. Predoi-Cross, M. Rotger, A.A. Ruth, S.S. Yu, K. Sung, S.A. Tashkun, J. Tennyson, V.I. Tyuterev, J. Vander Auwera, B.A. Voronin, A. Makie, The 2015 edition of the GEISA spectroscopic database, *J. Mol. Spectrosc.*, **327**, 31-72, (2016). Doi: [10.1016/j.jms.2016.06.007](https://doi.org/10.1016/j.jms.2016.06.007)
- <sup>26</sup> S. Wójtewicz, K. Stec, P. Masłowski, A. Cygan, D. Lisak, R.S. Trawiński, R. Ciuryło, Low pressure line-shape study of self-broadened CO transitions in the  $(3 \leftarrow 0)$  band, *JQSRT* **130**, 191-200, (2013). Doi: [10.1016/j.jqsrt.2013.06.005](https://doi.org/10.1016/j.jqsrt.2013.06.005)
- <sup>27</sup> Yu.G. Borkov, A.M. Solodov, A.A. Solodov, T.M. Petrova, E.V. Karlovets, V.I. Perevalov, Fourier transform CO spectra near  $1.6\ \mu\text{m}$ , *JQSRT* **253**, 107064 (2020). Doi: [10.1016/j.jqsrt.2020.107064](https://doi.org/10.1016/j.jqsrt.2020.107064)
- <sup>28</sup> K. Bielska, A. A. Kyuberis, Z.D. Reed, G. Li, A. Cygan, R. Ciuryło, E.M. Adkins, L. Lodi, Lorenzo, N.F. Zobov, V. Ebert, D. Lisak, J.T. Hodges, J. Tennyson, O.L. Polyansky, Subpromille Measurements and Calculations of



- CO (3←0) Overtone Line Intensities, *Phys. Rev. Lett.*, **129**, 043002 (2022). Doi: [10.1103/PhysRevLett.129.043002](https://doi.org/10.1103/PhysRevLett.129.043002)
- <sup>29</sup> Z.D. Reed, H. Tran, H.N. Ngo, J.-M. Hartmann, J.T. Hodges, Effect of Non-Markovian Collisions on Measured Integrated Line Shapes of CO. *Phys. Rev. Lett.* **130**(14), 143001 (2023), Doi: [10.1103/PhysRevLett.130.143001](https://doi.org/10.1103/PhysRevLett.130.143001)
- <sup>30</sup> Q. Huang, Y. Tan, R.-H. Yin, Z.-L. Nie, J. Wang, S.-M. Hu, Line intensities of CO near 1560 nm measured with absorption and dispersion spectroscopy. *Metrologia* **61**(6), 065003 (2024). Doi [10.1088/1681-7575/ad7ec0](https://doi.org/10.1088/1681-7575/ad7ec0)
- <sup>31</sup> S.A. Tashkun, V.I. Perevalov, R.R. Gamache, J. Lamouroux, "CDSD-296, high resolution carbon dioxide spectroscopic databank: Version for atmospheric applications", *JQSRT* **152**, 45-73 (2015). Doi: [10.1016/j.jqsrt.2014.10.017](https://doi.org/10.1016/j.jqsrt.2014.10.017)
- <sup>32</sup> S.A. Tashkun, V.I. Perevalov, R.R. Gamache, J. Lamouroux, "CDSD-296, high-resolution carbon dioxide spectroscopic databank: An update", *JQSRT*. **228**, 124–131 (2019). Doi: [10.1016/j.jqsrt.2019.03.001](https://doi.org/10.1016/j.jqsrt.2019.03.001)
- <sup>33</sup> L.D. Tubbs, D. Williams, "Broadening of Infrared Absorption Lines at Reduced Temperatures: Carbon Dioxide", *J. Opt. Soc. Am.* **62**(2), 284-289 (1972). Doi: [10.1364/JOSA.62.000284](https://doi.org/10.1364/JOSA.62.000284)
- <sup>34</sup> M. Wahlen, R.S. Eng, K.W. Nill, "Tunable diode laser spectroscopy of <sup>14</sup>CO<sub>2</sub>: absorption coefficients and analytical applications", *Appl. Opt.* **16**, 2350–2352 (1977). Doi: [10.1364/AO.16.002350](https://doi.org/10.1364/AO.16.002350)
- <sup>35</sup> B. Fridovich, W.C. Braun, G.R. Smith, E.E. Champion, "Strengths of single lines in the <sup>12</sup>C<sup>16</sup>O<sub>2</sub>, v<sub>3</sub> band at 4.3 μm", *J. Mol. Spectrosc.* **81**(1), 248–255 (1980). Doi: [10.1016/0022-2852\(80\)90341-0](https://doi.org/10.1016/0022-2852(80)90341-0)
- <sup>36</sup> C.P. Rinsland, A. Baldacci, K. Narahari Rao, "Strengths of <sup>13</sup>C<sup>16</sup>O<sub>2</sub> Lines at 4.3 μm", *J. Mol. Spectrosc.* **81**(1), 256–261 (1980). Doi: [10.1016/0022-2852\(80\)90342-2](https://doi.org/10.1016/0022-2852(80)90342-2)
- <sup>37</sup> V. Malathy Devi, B. Fridovich, G.D. Jones, D.G.S. Snyder, "Diode Laser Measurements of Strengths, Half-Widths, and Temperature Dependence of Half-Widths for CO<sub>2</sub> Spectral Lines near 4.2 μm", *J. Mol. Spectrosc.* **105**(1), 61–69 (1984). Doi: [10.1016/0022-2852\(84\)90103-6](https://doi.org/10.1016/0022-2852(84)90103-6)
- <sup>38</sup> C. Cousin, R. Le Doucen, J.P. Houdeau, C. Boulet, A. Henry, "Air broadened linewidths, intensities, and spectral line shapes for CO<sub>2</sub> at 4.3 μm in the region of the AMTS instrument", *Appl. Opt.* **25**, 2434–2439 (1986). Doi: [10.1364/AO.25.002434](https://doi.org/10.1364/AO.25.002434)
- <sup>39</sup> J.W.C. Johns, "Absolute intensity and pressure broadening measurements of CO<sub>2</sub> in the 4.3-μm region", *J. Mol. Spectrosc.* **125**(2), 442–464 (1987). Doi: [10.1016/0022-2852\(87\)90109-3](https://doi.org/10.1016/0022-2852(87)90109-3)
- <sup>40</sup> L. Rosenmann, M.Y. Perrin, J. Taine, "Collisional broadening of CO<sub>2</sub> IR lines. I. Diode laser measurements of CO<sub>2</sub>-N<sub>2</sub> mixtures in the 295–815 K temperature range", *J. Chem. Phys.* **88**, 2995–2998 (1988). Doi: [10.1063/1.453940](https://doi.org/10.1063/1.453940)
- <sup>41</sup> J.W.C. Johns, "Absolute intensities in CO<sub>2</sub>: the 4.3- and 2.7 μm regions revisited", *J. Mol. Spectrosc.* **134**(2), 433–439 (1989). Doi: [10.1016/0022-2852\(89\)90328-7](https://doi.org/10.1016/0022-2852(89)90328-7)
- <sup>42</sup> L. Rosenmann, S. Langlois, C. Delaye, J. Taine, "Diode Laser Measurements of CO<sub>2</sub> Line Intensities at High Temperature in the 4.3 μm Region", *J. Mol. Spectrosc.* **149**(1), 167–184 (1991). Doi: [10.1016/0022-2852\(91\)90151-Y](https://doi.org/10.1016/0022-2852(91)90151-Y)
- <sup>43</sup> L. Rosenmann, S. Langlois, J. Taine, "Diode Laser Measurements of CO<sub>2</sub> Hot Band Line Intensities at High Temperature near 4.3 μm", *J. Mol. Spectrosc.* **158**(2), 263–269 (1993). Doi: [10.1006/jmsp.1993.1070](https://doi.org/10.1006/jmsp.1993.1070)
- <sup>44</sup> P.J. Medvecz, K.M. Nichols, "Experimental Determination of Line Strengths for Selected Carbon Monoxide and Carbon Dioxide Absorption Lines at Temperatures between 295 and 1250 K", *Appl. Spec.* **48**(11), 1442–1450 (1994). Doi: [10.1366/0003702944028074](https://doi.org/10.1366/0003702944028074)
- <sup>45</sup> J.L. Teffo, C. Claveau, A. Valentin, "Infrared fundamental bands of O<sup>13</sup>C<sup>17</sup>O isotopic variants of carbon dioxide", *JQSRT* **59**(3–5), 151–164 (1998). Doi: [10.1016/S0022-4073\(97\)00109-X](https://doi.org/10.1016/S0022-4073(97)00109-X)
- <sup>46</sup> C. Claveau, J.L. Teffo, D. Hurtmans, A. Valentin, "Infrared Fundamental and First Hot Bands of O<sup>12</sup>C<sup>17</sup>O Isotopic Variants of Carbon Dioxide", *J. Mol. Spectrosc.* **189**(2), 153–195 (1998). Doi: [10.1006/jmsp.1998.7546](https://doi.org/10.1006/jmsp.1998.7546)
- <sup>47</sup> R.A. Toth, C.E. Miller, L.R. Brown, V. Malathy Devi, D. Chris Benner, Line strengths of <sup>16</sup>O<sup>13</sup>C<sup>16</sup>O, <sup>16</sup>O<sup>13</sup>C<sup>18</sup>O, <sup>16</sup>O<sup>13</sup>C<sup>17</sup>O and <sup>18</sup>O<sup>13</sup>C<sup>18</sup>O between 2200 and 6800 cm<sup>-1</sup>, *J. Mol. Spectrosc.* **251**(1), 64-89 (2008). Doi: [10.1016/j.jms.2008.01.009](https://doi.org/10.1016/j.jms.2008.01.009)

- <sup>48</sup> D. Jacquemart, F. Gueye, O.M. Lyulin, E.V. Karlovets, D. Baron, V.I. Perevalov, "Infrared spectroscopy of CO<sub>2</sub> isotopologues from 2200 to 7000 cm<sup>-1</sup>: I – Characterizing experimental uncertainties of positions and intensities", *JQSRT* **113**, 961–975 (2012). Doi: [10.1006/jqsrt.2012.02.020](https://doi.org/10.1006/jqsrt.2012.02.020)
- <sup>49</sup> E. Zak, J. Tennyson, O. L. Polyansky, L. Lodi, N. F. Zobov, S. A. Tashkun, V. I. Perevalov, A room temperature CO<sub>2</sub> line list with ab initio computed intensities, *JQSRT* **177**, 31-42 (2016). Doi: [10.1016/j.jqsrt.2015.12.022](https://doi.org/10.1016/j.jqsrt.2015.12.022)
- <sup>50</sup> C.M. Deeley, J.W.C. Johns, Absolute intensities of CO<sub>2</sub> bands in the 2.7-μm region, *J. Mol. Spectrosc.* **129**(1), 151-159 (1988). Doi: [10.1016/0022-2852\(88\)90266-4](https://doi.org/10.1016/0022-2852(88)90266-4)
- <sup>51</sup> V.M. Devi, D.C. Benner, C. P. Rinsland, M. A-H Smith, Absolute rovibrational intensities of <sup>12</sup>C<sup>16</sup>O<sub>2</sub> absorption bands in the 3090–3850 cm<sup>-1</sup> spectral region, *JQSRT* **60**(5), 741-770 (1998). Doi: [10.1016/S0022-4073\(98\)00080-6](https://doi.org/10.1016/S0022-4073(98)00080-6)
- <sup>52</sup> F. André, M.Y. Perrin, J. Taine, FTIR measurements of <sup>12</sup>C<sup>16</sup>O<sub>2</sub> line positions and intensities at high temperature in the 3700–3750 cm<sup>-1</sup> spectral region, *J. Mol. Spectrosc.* **228**(1), 187-205 (2004). Doi: [10.1016/j.jms.2004.07.004](https://doi.org/10.1016/j.jms.2004.07.004)
- <sup>53</sup> Farooq, A., Jeffries, J. & Hanson, R. CO<sub>2</sub> concentration and temperature sensor for combustion gases using diode-laser absorption near 2.7 μm. *Appl. Phys. B* **90**, 619–628 (2008). Doi: [10.1007/s00340-007-2925-y](https://doi.org/10.1007/s00340-007-2925-y)
- <sup>54</sup> A. Pogány, O. Ott, O. Werhahn, V. Ebert, Towards traceability in CO<sub>2</sub> line strength measurements by TDLAS at 2.7μm, *JQSRT* **130**, 147-157 (2013). Doi: [10.1016/j.jqsrt.2013.07.011](https://doi.org/10.1016/j.jqsrt.2013.07.011)
- <sup>55</sup> R.A. Toth, C.E. Miller, L.R. Brown, V. Malathy Devi, D. Chris Benner, Line positions and strengths of <sup>16</sup>O<sup>12</sup>C<sup>18</sup>O, <sup>18</sup>O<sup>12</sup>C<sup>18</sup>O and <sup>17</sup>O<sup>12</sup>C<sup>18</sup>O between 2200 and 7000 cm<sup>-1</sup>, *J. Mol. Spectrosc.* **243**(1), 43-61 (2007). Doi: [10.1016/j.jms.2007.03.005](https://doi.org/10.1016/j.jms.2007.03.005).
- <sup>56</sup> A.V. Domanskaya, R.E. Asfin, A.A. Kyuberis, V. Ebert, "CH<sub>4</sub> broadening and shifting coefficients in the Fermi triad of <sup>12</sup>C<sup>16</sup>O<sub>2</sub> in the 2 μm region". *JQSRT* **235**, 209-216 (2019). doi: [10.1016/j.jqsrt.2019.07.004](https://doi.org/10.1016/j.jqsrt.2019.07.004)
- <sup>57</sup> R.A. Toth Measurements of positions, strengths, and self-broadened widths of H<sub>2</sub>O from 2900 to 8000 cm<sup>-1</sup>: line strength analysis of the 2nd triad bands, *JQSRT* **94**(1), 51-107 (2005). doi: [10.1016/j.jqsrt.2004.08.042](https://doi.org/10.1016/j.jqsrt.2004.08.042).
- <sup>58</sup> Radu M. Mihalcea, Douglas S. Baer, and Ronald K. Hanson, Diode-laser absorption measurements of CO<sub>2</sub> near 2.0 μm at elevated temperatures *Appl. Opt.* **37**, 8341-8347 (1998). doi: [10.1364/ao.37.008341](https://doi.org/10.1364/ao.37.008341).
- <sup>59</sup> Corsi, C., D'Amato, F., De Rosa, M. et al. High-resolution measurements of line intensity, broadening and shift of CO<sub>2</sub> around 2 μm. *Eur. Phys. J. D* **6**, 327–332 (1999). Doi: [10.1007/s100530050316](https://doi.org/10.1007/s100530050316).
- <sup>60</sup> J. Geng, J. I. Lunine, and G. H. Atkinson, Absolute intensities, and pressure-broadening coefficients of 2-μm CO<sub>2</sub> absorption features: intracavity laser spectroscopy., *Appl. Opt.* **40**, 2551-2560 (2001). Doi: [10.1364/AO.40.002551](https://doi.org/10.1364/AO.40.002551)
- <sup>61</sup> M. E. Webber, J. Wang, S. T. Sanders, et al., In situ combustion measurements of CO, CO<sub>2</sub>, H<sub>2</sub>O and temperature using diode laser absorption sensors. *Proceedings of the Combustion Institute*, **28**(1) 407-413 (2000) [10.1016/S0082-0784\(00\)80237-4](https://doi.org/10.1016/S0082-0784(00)80237-4)
- <sup>62</sup> V. Zéninari, A. Vicet, B. Parvitte, L. Joly, G. Durry In situ sensing of atmospheric CO<sub>2</sub> with laser diodes near 2.05 μm: a spectroscopic study." *Inf. Phys. and Tech.* **45**(3) 229-237 (2004). Doi: [10.1016/j.infrared.2003.11.004](https://doi.org/10.1016/j.infrared.2003.11.004)
- <sup>63</sup> T. Le Barbu, V. Zéninari, B. Parvitte, D. Courtois, G. Durry, Line strengths and self-broadening coefficients of carbon dioxide isotopologues (<sup>13</sup>CO<sub>2</sub> and <sup>18</sup>O<sup>12</sup>C<sup>16</sup>O) near 2.04 μm for the in-situ laser sensing of the Martian atmosphere, *JQSRT* **98**(2), 264-276 (2006). [10.1016/j.jqsrt.2005.05.089](https://doi.org/10.1016/j.jqsrt.2005.05.089)
- <sup>64</sup> R.A. Toth, L.R. Brown, C.E. Miller, V. Malathy Devi, D. Chris Benner Line strengths of <sup>12</sup>C<sup>16</sup>O<sub>2</sub>: 4550–7000 cm<sup>-1</sup> *J. Mol. Spectrosc.* **239**(2), 221-242 (2006). Doi: [10.1016/j.jms.2006.08.001](https://doi.org/10.1016/j.jms.2006.08.001)
- <sup>65</sup> L. Régalia-Jarlot, V. Zéninari, B. Parvitte, A. Grossel, X. Thomas, P. von der Heyden, G. Durry, A complete study of the line intensities of four bands of CO<sub>2</sub> around 1.6 and 2.0 μm: A comparison between Fourier transform and diode laser measurements, *JQSRT* **101**(2), 325-338 (2006). Doi: [10.1016/j.jqsrt.2005.11.021](https://doi.org/10.1016/j.jqsrt.2005.11.021).
- <sup>66</sup> L. Joly, F. Gibert et al. A complete study of CO<sub>2</sub> line parameters around 4845 cm<sup>-1</sup> for Lidar applications. *JQSRT* **109**(3), 426-434 (2008). Doi: [10.1016/j.jqsrt.2007.06.003](https://doi.org/10.1016/j.jqsrt.2007.06.003)





- <sup>82</sup> R. Hashemi, H. Rozario, A. Ibrahim, A. Predoi-Cross, "Line shape study of the carbon dioxide laser band I", *Can. J. Phys.* **91**, 924-936 (2013). Doi: [10.1139/cjp-2013-0051](https://doi.org/10.1139/cjp-2013-0051)
- <sup>83</sup> Y. Tan, F. M. Skinner, S. Samuels, R. J. Hargreaves, R. Hashemi, I. E. Gordon, "H<sub>2</sub>, He, and CO<sub>2</sub> line-broadening coefficients, and temperature-dependence exponents for the HITRAN database. Part II: CO<sub>2</sub>, N<sub>2</sub>O, CO, SO<sub>2</sub>, OH, OCS, H<sub>2</sub>CO, HCN, PH<sub>3</sub>, H<sub>2</sub>S and GeH<sub>4</sub>", *Astrophys. J. Suppl. Series* **262** 40 (2022). Doi: [10.3847/1538-4365/ac83a6](https://doi.org/10.3847/1538-4365/ac83a6)
- <sup>84</sup> J.-M. Hartmann, "A simple empirical model for the collisional spectral shift of air-broadened CO<sub>2</sub> lines", *JQSRT* **110**, 2019-2026 (2009). Doi: [10.1016/j.jqsrt.2009.05.016](https://doi.org/10.1016/j.jqsrt.2009.05.016)
- <sup>85</sup> B. J. Drouin, D. C. Benner, L. R. Brown, M. J. Cich, T. J. Crawford, V. M. Devi, A. Guillaume, J. T. Hodges, E. J. Mlawer, D. J. Robichaud, F. Oyafuso, V. H. Payne, K. Sung, E. H. Wishnow, S. Yu, "Multispectrum analysis of the oxygen A-band", *JQSRT* **186**, 118-138 (2017). Doi: [10.1016/j.jqsrt.2016.03.037](https://doi.org/10.1016/j.jqsrt.2016.03.037)
- <sup>86</sup> D.A. Long, D.K. Havey, M. Okumura, C.E. Miller, J.T. Hodges, "O<sub>2</sub> A-band line parameters to support atmospheric remote sensing", *JQSRT* **111**(14), 2021-2036 (2010). Doi: [10.1016/j.jqsrt.2010.05.011](https://doi.org/10.1016/j.jqsrt.2010.05.011).
- <sup>87</sup> D. A. Long, D. J. Robichaud, J. T. Hodges, "Frequency-stabilized cavity ring-down spectroscopy measurements of line mixing and collision-induced absorption in the O<sub>2</sub> A-band", *J. Chem. Phys.* **137**(1), 014307 (2012). Doi: [10.1063/1.4731290](https://doi.org/10.1063/1.4731290)
- <sup>88</sup> D. J. Robichaud, J. T. Hodges, L. R. Brown, D. Lisak, P. Masłowski, L. Y. Yeung, M. Okumura, C. E. Miller, "Experimental intensity and lineshape parameters of the oxygen A-band using frequency-stabilized cavity ring-down spectroscopy", *J. Mol. Spectrosc.* **248**(1), 1-13 (2008). Doi: [10.1016/j.jms.2007.10.010](https://doi.org/10.1016/j.jms.2007.10.010)
- <sup>89</sup> D. J. Robichaud, L. Y. Yeung, D. A. Long, M. Okumura, D. K. Havey, J. T. Hodges, C. E. Miller, L. R. Brown, Experimental Line Parameters of the  $b^1\Sigma_g^+ \leftarrow X^3\Sigma_g^-$  Band of Oxygen Isotopologues at 760 nm Using Frequency-Stabilized Cavity Ring-Down Spectroscopy. *J. Phys. Chem. A* **113**(47), 13089-13099 (2009). DOI: [10.1021/jp901127h](https://doi.org/10.1021/jp901127h)
- <sup>90</sup> D.K. Havey, D.A. Long, M. Okumura, C.E. Miller, J.T. Hodges, "Ultra-sensitive optical measurements of high-J transitions in the O<sub>2</sub> A-band", *Chem. Phys. Lett.* **483**(1-3), 49-54 (2009). Doi: [10.1016/j.cplett.2009.10.067](https://doi.org/10.1016/j.cplett.2009.10.067)
- <sup>91</sup> D.A. Long, D.K. Havey, S.S. Yu, M. Okumura, C.E. Miller, J.T. Hodges, "O<sub>2</sub> A-band line parameters to support atmospheric remote sensing. Part II: The rare isotopologues" *JQSRT* **112** (16) 2527-2541 (2011). Doi: [10.1016/j.jqsrt.2011.07.002](https://doi.org/10.1016/j.jqsrt.2011.07.002)
- <sup>92</sup> D. A. Long, J. T. Hodges, , "On spectroscopic models of the O<sub>2</sub> A-band and their impact upon atmospheric retrievals", *J. Geophys. Res.* **117**, D12309 (2012). Doi: [10.1029/2012JD017807](https://doi.org/10.1029/2012JD017807)
- <sup>93</sup> A. Predoi-Cross, K. Hambrook, R. Keller, C. Povey, I. Schofield, D. Hurtmans, H. Over, G. Ch. Mellau, "Spectroscopic lineshape study of the self-perturbed oxygen A-band", *J. Mol. Spectrosc.* **248** (2), 85-110 (2008). Doi: [10.1016/j.jms.2007.11.007](https://doi.org/10.1016/j.jms.2007.11.007)
- <sup>94</sup> D. A. Long, D. K. Havey, M. Okumura, H. M. Pickett, C. E. Miller, and J. T. Hodges, Laboratory measurements and theoretical calculations of O<sub>2</sub> A band electric quadrupole transitions. *Phys. Rev. A*. **8**(4), 042513 (2009). Doi: [10.1103/PhysRevA.80.042513](https://doi.org/10.1103/PhysRevA.80.042513)
- <sup>95</sup> N. J. van Leeuwen, H. G. Kjaergaard, D. L. Howard, A. C. Wilson, Measurement of ultraweak transitions in the visible region of molecular oxygen. *J. Mol. Spectrosc.* **228**(1), 83-91 (2004). Doi: [10.1016/j.jms.2004.07.002](https://doi.org/10.1016/j.jms.2004.07.002)
- <sup>96</sup> K.J. Ritter, T.D. Wilkerson, High-resolution spectroscopy of the oxygen A band, *J. Mol. Spectrosc.* **121**(1), 1-19 (1987). Doi: [10.1016/0022-2852\(87\)90167-6](https://doi.org/10.1016/0022-2852(87)90167-6)
- <sup>97</sup> R. Schermaul, "Transition probability and line broadening for the  $b^1\Sigma_g^+(v=0) \leftarrow X^3\Sigma_g^-(v=0)$  band of the <sup>16</sup>O<sup>18</sup>O isotopomer of oxygen". *JQSRT* **62**(2), 181-191 (1999). Doi: [10.1016/S0022-4073\(98\)00102-2](https://doi.org/10.1016/S0022-4073(98)00102-2)
- <sup>98</sup> R.C. Schermaul, M. Learner, "Precise line parameters and transition probability of the atmospheric A band of molecular oxygen <sup>16</sup>O<sub>2</sub>", *JQSRT* **61**(6), 781-794 (1999). Doi: [10.1016/S0022-4073\(98\)00066-1](https://doi.org/10.1016/S0022-4073(98)00066-1)
- <sup>99</sup> L.R. Brown, C. Plymate, "Experimental Line Parameters of the Oxygen A Band at 760 nm", *J. Mol. Spectrosc.* **199**(2), 166-179 (2000). Doi: [10.1006/jmsp.1999.8012](https://doi.org/10.1006/jmsp.1999.8012)
- <sup>100</sup> B. Anderson, R. Brecha, "Tunable diode laser absorption measurement of oxygen A-band line strengths", *Appl. Phys. B* **87**, 379-385 (2007). Doi: [10.1007/s00340-007-2581-2](https://doi.org/10.1007/s00340-007-2581-2)